**UNIVERSITY OF OSLO**
**Department of Geosciences - MetOs section.**

# Precipitation in southern Africa: dynamical downscaling of CAM using WRF

Master thesis in Geosciences Meteorology and Oceanography

Anna von Streng Velken

**1st June 2011**

## Abstract

Regional climate modeling has become an important tool for downscaling global climate models (GCMs), to assess high impact regional climate projections. Southern Africa is one of the most exposed regions to the effects of climate change, as it is highly depended on rain fed agriculture. Nevertheless, there are only a handful of regional climate studies previously performed in southern Africa.

In this thesis, the Weather and Research Forecast (WRF) model's performance as a dynamical downscaler for the Community Atmospheric Model (CAM) in southern Africa is investigated, focusing on precipitation patterns over the time period of 1990-2009. The domain covers southern Africa from 5°-38° S and 8°-53° E with a resolution of 27 km x 27 km and 36 vertical layers. WRF is initialised by CAM and Community Land Model (CLM) data, and forced every 6hours by SSTs and lateral boundary conditions from CAM. Seasonal, annual, interannual and extreme events of precipitation in a historical run with WRF are outlined in this thesis. Additionally, a preliminary study of downscaling a future time slice (2050-2069) is performed. The results from the historical run have been validated with satellite observational data.

WRF reproduces the mean seasonal and annual precipitation cycle satisfactorily, although overestimating in the summer months in the Indian Ocean and over the southern African plateau. The latter is probably caused by a too strong low-level convergence in WRF, leading to a stronger Walker circulation and positive precipitation feedback mechanism over the southern African plateau. Compared to satellite observations, WRF generally provides slightly better results concerning mean precipitation than CAM. Testing different physical scheme combinations (cumulus parametrization and planetary boundary layer) in shorter runs imply that in some areas the the overestimation of precipitation can be reduced with alternative scheme options, although attaining biases in other regions. The correlations between observed seasonal means and CAM/WRF are computed over selected regions, showing that the interannual variability is generally poorly captured by both models, although somewhat better over a few regions in CAM. The results suggest that SST anomalies are not the governing driving force behind interannual variability over most parts of southern Africa. WRF's applicability for computing extreme precipitation changes over a time period is briefly discussed, and WRF seems to adequately reproduce the precipitation changes compared to TRMM (for 1998-2009).

To the degree this study can be compared with previous, the results are well in line with former work. As in previous studies the wet summer precipitation bias in the RCM (WRF) is similar to the GCM (CAM) over southern Africa. However, WRF generally reproduces seasonal precipitation somewhat closer to observed values compared to CAM, and

sensitivity studies suggest the biases might be further diminished by changing the physical parametrization through alternative scheme options. Thus this study seems to be a step in the right direction for dynamically downscaling of GCMs over southern Africa and motivates for further research.

## Acknowledgement

Consuming all my time, energy and thoughts lately, it is surreal to write the final words of my thesis. There are many people that deserves to be mentioned here! First, I would like to thank Frode Stordal, my co-supervisor, for an intersting aim of study. Thanks for truly inspiring discussions and enthusiasm that infects. Many thanks also to my supervisor, Terje Berntsen, for helpfull discussions of results, valuable suggestions, and even looking at drafts while tenting in the mountains.

This thesis has been a technical challenge and many people have been contributing. Without Sandeep Sukumaran, this study would not have been possible to perform. He has been of great help providing CAM outputs, and he has an enormous patients with a master student that might ask the same questions twice. Gunnar Wollan has been of great support, especially concerning TITAN problems and acute saving space issues etc. Also thanks to Cindy Bruyere at NCAR, Torleif Markussen Lunde, Ulla Heikkilä and Michel Mesquita at Bjerknes Center andLluis Fita Borrell at Santader Meteorology Group for great technical help with WRF through mail correspondence. Additionally I want to thank Øivind Hodnebrog at UiO, for general help and support.

In addition to working with a truly interesting thesis (although consuming too much time lately so one tends to forget), it is my friends and fellow students that have made this year so great; thank you! Thanks to "Metos-Forskningsparken Foosball Association" for a first half year that was not all about the thesis. Thanks to "the golder rack" coping with a talkative Bergenser, whom have taken up all the space around us lately. My friends outside of geophysics have also coped with thesis complaints, and specially thanks to Camilla and Ingvild, who always, always!! makes me laugh and are supportive, no matter what. Kristin, thanks for coffee breaks and cheerfull text messages! Thanks to OSI basketball for overall making my student life a blast.

I want to thank my family for being there for me, and specially my sister Ingrid; thanks for all your support and for proofreading my thesis. Last but definitely not least: my boyfriend and partner in life - thanks for still being that, and for your always amazing patients.

Oslo, June 1, 2011
Anna von Streng Velken

# Contents

# Chapter 1

# Introduction

Africa is one of the most vulnerable continents when it comes to the consequences of climate change. With a high dependency on agriculture, poor human health and water insecurity, Africa is especially sensitive to the projected changes of global warming (Stringer et al., 2009).

Despite little contribution to the global increase of greenhouse gases, the most indigent countries will experience the largest consequences of a changing climate. Malawi is one of these, being among the poorest countries

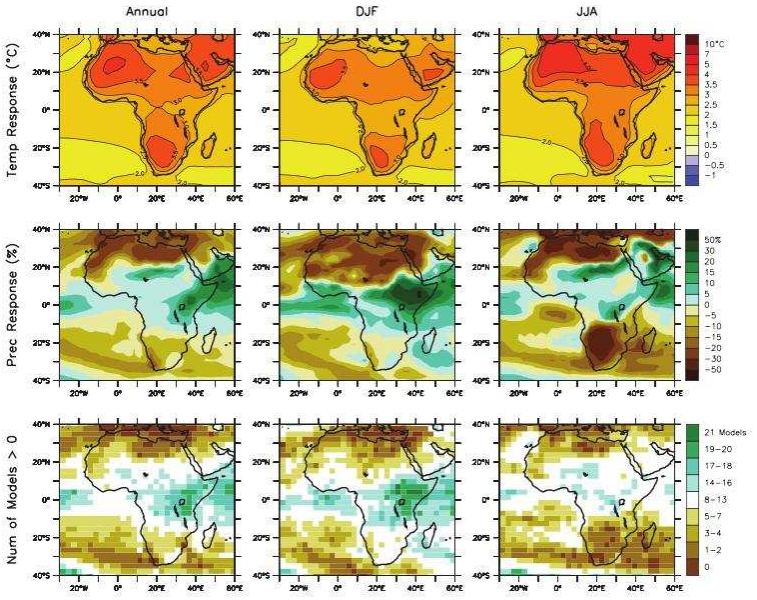


**Figure 1.1:** *Temperature and precipitation changes over Africa from the MMD-A1B simulations in IPCC fourth assessment rapport. Top row: Annual mean, DJF (December, January, February) and JJA (June, July, August) temperature change between 1980 to 1999 and 2080 to 2099, averaged over 21 models. Middle row: same as top, but for fractional change in precipitation. Bottom row: number of models out of 21 that project increases in precipitation (Christensen et al., 2007).*

in southern Africa. 90 percent of Malawi's population lives in rural areas and relies on rain-fed agriculture on small scale holdings. Poor soil, undeveloped infrastructure, lack of education and low level of climate change awareness for decision makers are some of the factors that detains climate adaptation and mitigation in undeveloped regions (Stringer et al., 2009).

## 1.1 Why downscaling over southern Africa ?

"All models are wrong, but some are useful"
(George E. P. Box)

Global Climate Models (GCMs) can provide a sufficient estimation of the climate on a global scale. With constrained computational resources, the GCMs are forced to run on a coarse grid (typically 125 -400km) as they represent the entire globe. Therefor, GCMs will not be able to capture details needed on a national level. The processes driven by surface interaction, like extreme rainfall events or tropical cyclones, will be poorly described by a GCM. Thus, dynamically downscaling of global climate models has become an increasingly popular research subject the past few decades.

When downscaling large scale fields from GCMs, generally four types of methods can be utilised. One is the application of a simple interpolation of the GCM results to a finer resolution. Another is to do a statistical downscaling using empirical relationship between a large - and small scale climate, computing the relationship between the two scales from observational climate data. A third method involves running GCM for a short time slice with higher resolution. Lastly, one can nest a regional climate model within a GCM. The latter will be performed in this study. The first two methods are not as computationally heavy as the others, but the interpolation is difficult to apply for other purposes than mean climate and the empirical downscaling is a comprehensive and difficult task over large areas. Running GCM on a high resolution grid is extremely computationally expensive and the originally physical schemes might not be a good representation for the local climate, in addition to being restricted to a short time period (Arnell et al., 2003).

RCMs have lately become a well used tool for downscaling. Only simulating a specific area, RCMs can run with higher resolution (typically less than 10-80km) and output shorter temporal results (daily, hourly or less). The thought is that variables like precipitation and surface air temperature will be more precisely simulated by a RCM, as it represent complex terrain, coastlines and lakes more accurately (Giorgi and Mearns, 1991; Caldwell et al., 2009). For a short time-slice looking at specific episodes or incidents, RCMs can provide thorough information on a local level running with resolution down to or even less than 1km. A RCM

is usually initialized and forced on the lateral boundaries by a GCM, sea surface temperature (SST) and initial land-surface conditions for a chosen region.

Analysing of results from RCMs run can be of value on a stand alone basis, but the daily high resolution outputs are also important driving-fields for hydrology models. Hydrology models can provide better knowledge of the climate change feedback on the cryosphere, biosphere and landsurface. They can provide improved estimations of the two very fundamental climate change feedback processes involving water vapor and clouds (Davies and Simonovic, 2005). Output from RCMs and hydrology models are both necessary to identify the impacts of climate change that is relevant on a societal level. Such projections on a regional scale can provide guiding for policy makers within economy, water supply, agriculture, health, etc (Boko et al., 2007).

According to Christensen et al. (2007) the temperature in Africa is likely to rise by 3 to 4 $^{\circ}$ C within the next century, with less warming in equatorial and coastal regions. Rainfall patterns are more uncertain, but it is likely to see changes in precipitation in the southern parts, especially in the winter rainfall (see figure 1.1). The rainfall regime in southern Africa today is characterized by great variability at various time scales from intraseasonal and interannual to decadal and multidecadal. Although local people of southern Africa are no strangers to climate variability, a large change in the rainfall patterns and more extreme events can be severely damaging, especially for less developed countries like Malawi. Low food security combined with population growth can be devastating to the population in these regions.

GCMs are known to have significant errors, in particular over Africa. In the multi-model data set (MMD) used in IPCC, 90 % of the models overestimate precipitation in southern Africa(Christensen et al., 2007). It is clearly a need for better precipitation estimations, but to which extent regional climate models can improve the simulations of rainfall over Africa is still somewhat unclear. Regional climate modelling involves large uncertainties, especially concerning three main issues: The physical and dynamical processes being discretizised and described by the model, the inaccuracy in the forcing data from the GCM (which influences the RCMs strongly) and the uncertainties in the future emission scenarios. Thus RCMs will not predict an exact solution to how the future climate is going to change. RCMs are used as a tool to provide a hypothesis of what to expect for the future climate. Regional climate modelling is not intended to modify or correct the large scale circulation models, but to add additional details of topography, land-surface and advanced representation of the physics and dynamics. It is a technical challenge to choose the right boundary conditions, domain placement and size to avoid large discrepanicies between have the large scale physics and dynamics in the global model, and the small scale representation in the regional model.

Regional climate runs are highly valuable when they can be compared to other RCMs and together compose ensemble, thus studies like this are important in the process of making an assumption on how the climate will change (Engelbrecht et al., 2008; Lo et al., 2008). A reliable projection is especially valuable for communities that do not have the resources to act fast to considerable climate changes.

This study will downscale the Community Atmosphere Model (CAM). The data is provided by Sandeep Sukumaran working on the SoCoCa-project[1] lead by the University of Oslo. The Weather Research and Forecast model[2] (WRF) is used as a dynamical downscaler in this study. WRF is currently used by over 13 000 scientists all over the world (Holland et al., 2011)

## 1.2 Previous work

Climate modeling started to develop for real in the 1970s, running on a coarse grid around 5°-7.5°. As the climate change topic was brought more and more to an international attention, the need to resolve processes on a smaller scale became evident. Dickinson et al (1989) and Giorgi (1990) was ground-breaking in their work on forming a base for limited-area models (LAM), the first towards regional climate modelling. In the last two decades RCMs has been applied in several studies all over the world, though mostly in the northern hemisphere where the technical capacity is stronger (Tummon, 2011).

According to Christensen et al. (2007) regional climate studies in other parts of the world show that RCMs generally improve the wet bias in GCMs. An exception is southern Africa, where the biases in RCMs are reminiscent to the global models. The semi-arid areas of southern Africa seem to enhance the regional climate sensitivity. Thus regional climate modelling in southern Africa is especially sensitive to domain size, lateral boundary forcing, physical parametrizations etc., which is demonstrated by the varying results from previous studies using RCMs in southern Africa (Hudson and Jones, 2002; Engelbrecht et al., 2008; Tadross et al., 2005; Arnell et al., 2003; Cretat et al., 2011; Sylla et al., 2011; Giorgi et al., 2011). As part of a larger regional climate study over southern Africa, Hudson and Jones (2002) computed two 15 year long historical simulations forcing with different lateral boundary conditions: one given by GCM and

[1] Socioeconomic Consequences of Climate Change in Sub-equatorial Africa (SoCoCa) is a project lead by Frode Stordal at the University of Oslo, using regional climate modelling for input in hydrology models and eventually looking at the economical consequences of climate change for southern Africa. CAM is the atmospheric model component of NCAR's Community Climate System Model (CCSM). CCSM is one of the leading models used by IPCC

[2] See chapter 3 for technical description of WRF

the other by reanalysis data. Both aggravated the precipitation bias compared to the GCM when looking at area-averaged means over summer[3]. The overestimation of summer precipiation over southern Africa is generally an issue in previous studies. However, in 2011 Cretat et al. looked at summer season pecipiation over southern Africa, by performing sensitivty studies over a specific summer seson using various physical parameterizations in WRF, to find substansially variable results, some also containing large dry biases.

Previous studies using WRF as a regional climate model in the U.S indicates that the spacial distribution and extreme events of precipitation are well captured. However WRF also seems to overpredict the rainfall rate in general, especially in mountain regions (Caldwell et al., 2009; Qian et al., 2010; Bukovsky and Karoly, 2009; Bell et al., 2003). The method of downscaling WRF by CAM is in its early stage [4]. To the author's knowledge there are no former studies focusing on southern Africa providing WRF with lateral boundary conditions from CAM.

## 1.3 Description of the study

This study mainly concentrate on a historical run, however its primary purpose is that the dynamically downscaling can eventually be used to compare a present and a future run, to analyse possible climate change signals. Using this technique of comparison, we have made the assumption that the biases developing from the physics in the two runs are small compared to the differences that will evolve from the forcing of SSTs and greenhouse gases. Thus the main difference will possibly not arise from model errors, but represent the climate change it self. It has therefor been stressed throughout the work, that the intital and driving conditions of the future and the present run should be as similar as possible. Hence, the historical run has not been nudged against observations[5]. The forcing of the historical and future run are therefor only distinguished by different SSTs (observed vs modelled) and input of greenhouse gases. Nevertheless, it is important to have in mind that errors of present day simulations may produce a forcing in the future run that needs to be considered when analysing. Thus extensive sensitivity studies in advance of computing longer simulations are recommended, but were not performed is this thesis because of time limitations.

[3] In Hudson and Jones 2002, area-avergad precipitation over land areas are 60% higher in downscaled GCM data (HadAM3H) by RCM (HadRM3H), 52% higher for RCM dowscaling of reanalysis data (ERA-40) and 39 % higher in the GCM itself compared to observed values

[4] In October 2003, NCAR supported the development of a regional climate modelling working group (group 16) to use WRF and CAM in order to address downscaling and upscaling issues in climate modelling

[5] Nudging consists of terms added to the prognostic equations, which nudges the solutions towards observations (or other forcing data)

As WRF is applied for daily weather forecasting, modifications has been performed before running it as a regional climate model (see section 3.3 Chapter 3). WRF as a dynamical downscaler is becoming popular, though not extensively utilised for regional climate simulations and especially not by forcing with CAM. Thus, documentation concerning this is rather sparse, and resulted in time consuming technical challenges (see Chapter 3, section 3.4 for a short description).

The main objective for this thesis is to evaluate WRF's ability to dynamically downscale CAM over southern Africa, by focusing on the precipitation patterns. The study will contribute as a member in an ensemble of RCMs and maybe even provide better estimations for some of the local physical processes. Similar downscaling of CAM (according to domain size and timeslice) will be computed using RegCM3[6] associated with the SoCoCa-project. Thus a secondary purpose of this study is to provide comparable datasets utilising WRF. A third objective is to eventually supply input data for hydrology models in the SoCoCa project. Hydrology models are depended on high resolution, high quality data of surface variables (precipitation, wind, temperature, relative humidity) on a daily basis.

WRF is initialised by CAM and land surface data from CLM[7], and forced by SSTs and at the lateral boundaries by CAM. We focus on a historical run from 1990-2009 and have made testruns for a future period from 2050-2069, using RCP4.5 scenarios from IPCC [8]. For validation of the historical run, WRF and CAM are compared to observational satellite data. In general, this thesis will provide an evaluation of how WRF preforms as a regional climate model in southern Africa.

The thesis is organised as follows: First a short background on precipitation patterns, climate changes and agriculture in southern Africa is presented in the next chapter (Chapter 2). Then a thorough description of WRF and the model setup is given in the methodology chapter (Chapter 3). Next results are provided in Chapter 4 along with suggestions for future work. Finally in Chapter 5, a summary and conclusion remarks are given.

[6]RegCM3 is a 3-dimensional, sigma-coordinate, hydrological primitive equation regional climate model, developed by scientists inside and outside of PWC/ICTP (`http://users.ictp.it/RegCNET/model.html`)

[7]Community Land Model (CLM) is the land model in CCSM.

[8]The Representative Concentration Pathway (RCP) are new greenhouse-scenarios from the IPCC. RCP4.5 is a low-medium scenario of greenhouse gas emission(Moss et al., 2010). See Table A

# Chapter 2

# Background and motivation

This thesis focus on precipitation patterns to investigate WRF's abilities for downscaling CAM over southern Africa. An outline of the general weather systems are therefore needed. The motivation for this study is to contribute to the work that lays the ground for WRF as a RCM in southern Africa, and eventually provide climate change indices for decision makers. To accomplish this it is also important to understand what climate change is about, and how it is expected to affect the people of southern Africa. Thus in this chapter we will present an overview of the weather patterns in southern Africa today, why and how the climate is changing, and finally look at how the changes will affect the communities in southern Africa.

## 2.1 Atmospheric circulation and weather in southern Africa

Precipitation-producing systems are multiple and occur on various temporal and spatial scales. From synoptic cyclones or anticyclones, mesoscale thunderstorms and cumulus clouds to turbulence and cloud physics on a micro scale, the large and small scale processes and their interaction will determine the rainfall rate. Thus, the development of precipitation is complex and comprehensive, especially in southern Africa which stretches from tropical climate in the north to mid-latitude climate on the southern tip.

In this thesis Southern Africa is defined as the part of Africa south of 10 $^{\circ}$ S. It is a diverse region in many aspects; politically, culturally, ecologically and climatological (see figure 2.2[1]), making it an interesting and challenging area to study. There are many processes affecting the rainfall rates in southern Africa. Although important, all of them can not be studied in-depth in this thesis. An overview of the fundamental processes that

[1]Picture taken from `http://home.comcast.net/~rhaberlin/crpptnts.htm`


**Figure 2.1:** *The southern African countries.*

leads to precipitation in southern Africa is presented in this section. For a thorough understanding of the underlying circulations and interactions in southern Africa, "The Weather and Climate of Southern Africa " by Tyson and Preston-Whyte is recommended.

The main part of southern Africa is situated on a level of 1000 m.s.l, the so called southern African plateau, with narrow coastal margins around it in the south and southeast. There is a distinct change in the latitudinal distribution of precipitation, dividing the region in two parts. The northern part[2] is wet and humid with broad-leaf vegetation. The southern part[3] is semi-dry to dry and vegetated by fine-leafed savannas and grassland, with a semi-desert section in the south west (UNEP (2006); J. L Privette (2004); Tummon (2011)).

Most of southern Africa is located in the subtropics, where the descending air of the southern Hadley cell is dominant (see Figure 2.3[4]), resulting in primarily anticyclonic circulation patterns over the oceans in summer, and over the continent in the austral winter. This continental high pressure (Kalahari High Pressure) intensifies from May, preventing moist air to entrain over the continent, resulting in a dry and cool winter. While the Kalahari High Pressure expands, it also moves northward, giving the westerlies an opportunity to displace equatorwards.

During these dry and cool months from May through September in most of southern Africa, the moisture advection and convergence associated with

[2]Northern part is defined as : Angola, Malawi, Mozambique, Zambia and Zimbabwe, see Figure 2.1

[3]Southern part is defined as Botswana, Lesotho, Namibia, South-Africa and Swaziland

[4]Picture taken from `http://www.newmediastudio.org/DataDiscovery/Hurr_ED_Center/Easterly_Waves/Trade_Winds/Trade_Winds.html`

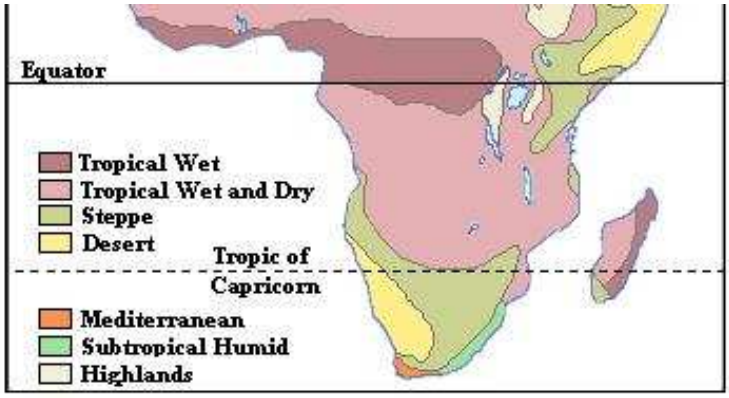


**Figure 2.2:** *The variety of African climates.*

the Inter Tropical Convergence Zone (ITCZ [5]) is situated in the northern hemisphere. Throughout the following months, starting from September the surface warms and the ITCZ moves southwards, bringing warmer and wetter conditions to southern Africa. This initiates the rainy season, which normally lasts from October to March. It is mainly in the rainy season that southern Africa receives its annual precipitation (90 % of the total annual precipitation).

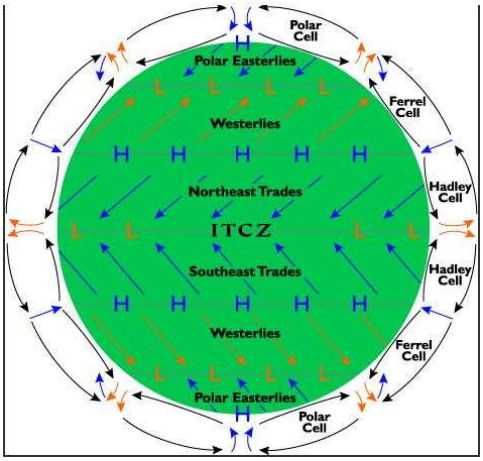


**Figure 2.3:** *Primary circulation cells and prevailing wind belts of Earth*

### 2.1.1 Geography and general weather producing systems

The southern tip of south Africa has an opposite climatology than the rest of the southern continent. Being situated closer to the mid-latitudes this region receives its small portion of rain in the austral winter. As the westerlies

[5]The convergence of the northern and southern Hadley cell

in the southern hemisphere strengthens and moves northwards (as mentioned above), they bring favorable conditions for convection when cold fronts and cut-off lows moves across the south and south west of southern Africa. The core of these westerlies reaches the southernmost point in the austral winter at 25° (Tyson and Preston-Whyte, 2000; Shugart et al., 2004).

The semi-permanent South Atlantic Anticyclone and the South Indian Anticyclone are the prevalent circulation patterns of southern Africa, being features of the high-pressure systems that dominate the subtropical belt. The shift in position for the South Atlantic Anticyclone can result in extended ridges breaking off in separate highs wondering into the westerlies and strongly affecting the weather in southern Africa. The seasonal east-west shifts of the Indian High affects the weather of the eastern parts of southern Africa.

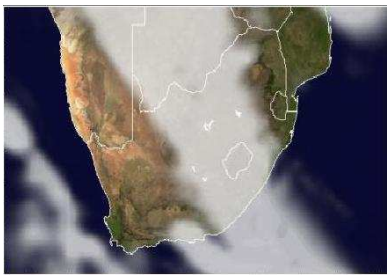

**Figure 2.4:** *Cloud bands stretching from the tropical north to the temperate south.*

From October a shallow heat low develops over Angola and northern Namibia and strengthens in January and February (when ITCZ is in its southern position). This Angolan low is the source of the tropical-temperate troughs (TTT), which is the most important rain-producing weather system of southern Africa in summer. As can be seen in figure 2.4[6], major cloud bands stretches from the tropics towards the mid-latitudes along the TTTs. This is the largest contributor for the annual rainfall on the southern African plateau (39 %). Escpecially when the ITCZ has a weak activity, the cloud bands effectively transfers heat and moisture from the tropics towards the mid-latitudes (Reason et al., 2006; Tyson and Preston-Whyte, 2000; Hart et al., 2010; Todd and Washington, 1999). Seasonal migration of the rainbands position can result in large local interannual changes of precipitation intensity(Christensen et al., 2007).

Tropical cyclones forming in the Indian Oceans can have a large impact on the rainfall rate off the eastern coast of Mozambique, west of Madagascar. During a summer season, usually between one and five storms pass between Madagascar and South Africa, normally re-curving and moving

[6]Picture taken from `http://www.myweather.co.za/weatherinfo/SAWeather.html`

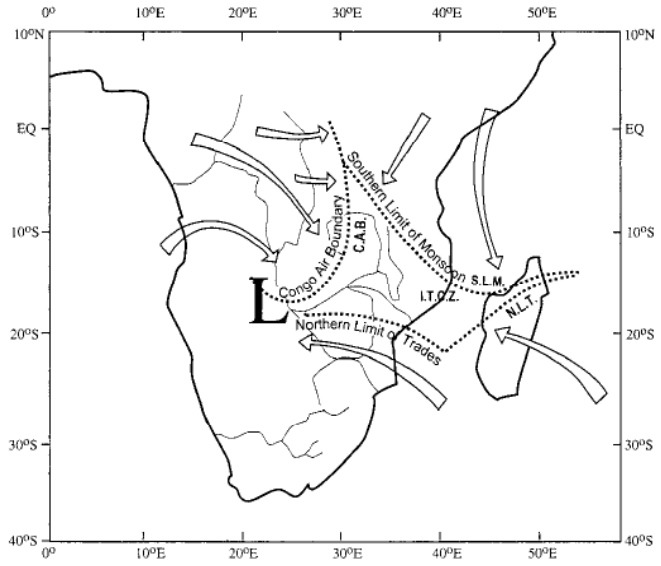


**Figure 2.5:** *The near surface airflow (arrows) and convergence zone (dashed lines) over southern Africa (McHugh and Rogers, 2001).*

along the Mozambique Channel[7]. Most of the cyclones occur in January or February, often associated with extensive rainfall and floods on the eastern coast. The storms dampen quickly over land, often leaving the central and western part of the plateau with normal rainfall conditions((Tyson and Preston-Whyte, 2000; Landman et al., 2005)).

### 2.1.2 Interannual variability

There is a high degree of interannual variability in southern Africa. A multitude of forcings are interacting; changing incidence, persistence and strength to form the great interannual variability over southern Africa(Reason et al., 2006). However, the scientists are not consenting to which degree each mechanism are influencing the interannual variability. Some of the processes thought to be of main influence will be shortly outlined in the following.

#### Displacement of ITCZ

As mentioned previously the ITCZ moves from the northern to the southern hemisphere over the year. Its average southern position (in the austral summer) is about 15-17 $^0$ S in the austral summer. Three different surface circulations tend to dominate in the summer months (DJF) to form

[7]The Mozambique Channel is the portion of Indian Ocean that lies between Mozambique and Madagascar.

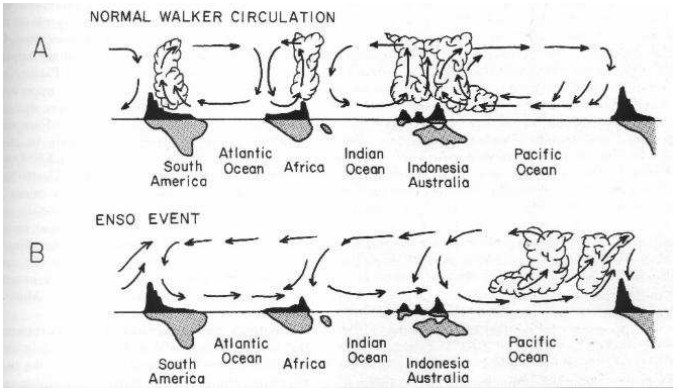


**Figure 2.6:** *The Walker circulation during non-ENSO (upper) and ENSO (El Nino, lower) events (Tyson and Preston-Whyte, 2000).*

the southeastern African convergence zone: Southeast trades from the Indian ocean, northeasterly monsoonal flow and westerly airstream over the Congo basin (Congo Air Boundary[8]), as demonstrated in Figure 2.5 (Hudson and Jones, 2002).

The three interacting flows can again be affected by pressure systems at higher altitude or tropical cyclones. They can also be inactive if little regional airflow convergence across them, resulting in displacement of the ITCZ. In extreme years the ITCZ can be situated near 10-12°S, leading to below average rainfall as the comparatively dry south-easterly trade winds dominates the circulation patterns. On the other extreme, the ITCZ can be displaced up to 20°S, resulting in anomalously moist air and heavy rainfall in these regions (McHugh and Rogers, 2001; Tummon, 2011).

### The Walker circulation

Continuity requires that each type of circulation has a counter part, either it is in the ocean or in the atmosphere. This results in coupled cyclones and anti-cyclones over the entire globe. A few of the larger pressure systems are more or less stationary and determines the daily weather by changing the paths of smaller anticyclones and cyclones. When these larger pressure systems get anomalously strong or weak, they can have significant impact the general weather systems.

In recent years there has been an increased focus on the coupling between the ocean and the atmosphere. The changes in the ocean happens on a longer time scale than in the atmosphere because of the higher heat capacity that the ocean holds, providing it with a longer "memory". This is of particular interest for researchers, as observations and prediction of marine conditions can be used to forewarn climatic consequences (Jury, 2002).

[8]Congo air boundary: humid, unstable and convergent air from the Congo basin.

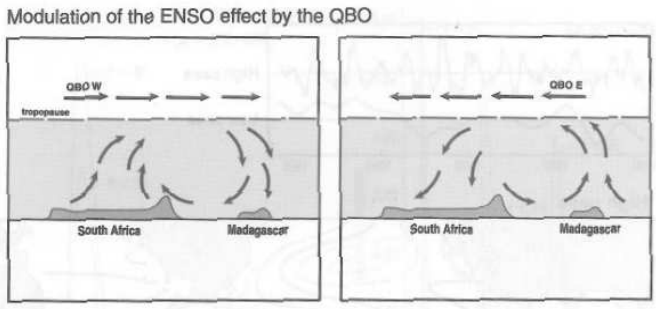


**Figure 2.7:** *The circulation over Southern Africa during ENSO event, when QBO is in its western and eastern phase. (Tyson and Preston-Whyte, 2000)*

Southern Africa has a high degree of interannual and interdecadal variability.

Most of the standing circulation cells are meridional (see Figure 2.3), but in the southern hemisphere there are a linked series of zonal cells which have important consequences for southern African weather: The Walker Circulation. It is caused by the changes in the sea surface temperatures in the Pacific Ocean and the inverse correlated lower-tropospheric pressure fields. The Walker circulation (see figure 2.7) can get displaced by changing SSTs over the eastern and western Pacific Ocean, setting up an atmospheric pressure difference over the Indian and Pacific Oceans called Southern Oscillation. In extreme phases this circulation is called ENSO (El Niño-Southern Oscillation), where in low phase (El Nino) there is a relatively high pressure over Indonesian regions and low pressure over the eastern Pacific, and in high phase (La Nina) the pressure gradient reverses resulting in the opposite regime (Tyson and Preston-Whyte, 2000).

For southern Africa, El Nino is mostly associated with extreme dry years[9]. One of the main causes is the land based cloud-bands that are relocated offshore. El Nino also entails a warmer Indian Ocean which strengthens the convection and release latent heat over the ocean, reducing the precipitation over land. In a non-ENSO year the cloud-bands are situated over southern Africa and the rainfall rate is anomalously high (Jury, 2002).

The ENSO signal over southern Africa is modified by the Quasi-Biennial Oscillation (QBO). QBO is a quasi-periodic reversal of winds in the equatorial stratosphere, fluctuating between an easterly and a westerly phase and is thought to interfere with the Walker circulation. In its westerly phase the Walker cell is reversed, resulting in the upper-level divergence followed by convection over southern Africa. Changing phase, the convection is suppressed over the subcontinent resulting in dry conditions (Mason and

[9]The southwestern tip of Southern Africa can experience wetter years during El Nino

Jury, 1997). ENSO seems to influence a greater percentage of the precipitation when the QBO is in its westerly phase, but this interaction is not jet thoroughly understood (Tyson and Preston-Whyte, 2000; Jury, 2002; Mason and Jury, 1997).

#### Antarctic Oscillation

For the western parts of South Africa, The Antarctic Oscillation (AAO) seems to influence the winter rainfall greatly. South of $20^0$S it is the prevailing circulation variability, characterized as positive (negative) when it is an anomalously negative (positive) pressure in the Antarctic and relatively positive (negative) pressure in the mid-latitudes (Reason and M.Rouault, 2005). A positive AAO can be associated with a strengthening of the westerlies and wetter winters for western South Africa. The negative phase results in a reverse condition. In 2005 Reason and Rouault found that the anomalies persisted into the spring season as well.

#### Anomalies in the Indian Ocean and Atlantic Ocean

Indian Ocean warm and cool events can occur independently of El Nino. As previously mentioned, the sea surface temperature over central equatorial Indian Ocean and the rainfall cycle over the subcontinent are in opposite phases, thus anomalously high SSTs results in under-average rainfall over southern Africa and vice verse. This correlation is nonlinear, and an increase in SSTs can also lead to enhanced rainfall as the Indian Ocean is the dominant source of moisture in the late summer rain . This is one of the features that GCMs seam to have difficulties simulating (Mason and Jury, 1997). The anomalies of the subtropical Indian and Atlantic Oceans are less understood. Below (above) average SSTs are implying dry (wet) conditions, possibly because of the effect on moisture fluxes in the overlying atmosphere, providing less (more) moisture to the troughs and ridging anticyclones (Mason and Jury, 1997).

## 2.2 Climate change

The cause of climate change is an external forcing that can influence and interact with the internal components of a climate system. The climate change that we are facing today, is forced by increasing greenhouse gases (GHG[10]). The Intergovernmental Panel on Climate Change (IPCC) fourth Assessment Report in 2007 concluded that global warming is occurring and that the increase in the global temperature is a result of human activities.

[10]H20 (water vapor), CO2, CH4, NO2, CFCs etc.

The greenhouse gas effect can be explained by the energy of the high intensity shortwave radiation from the sun being absorbed and emitted by the earth-atmosphere system in longwave radiation. A large portion of the thermal radiation is absorbed by the GHGs in the atmosphere and re-emitted to the earth, increasing the earths total received radiation and contributing to a higher surface temperature. Thus the impact of GHGs causes our planet's average temperature of 15 ° C (which would have been minus 18° C without them[11] (Hartmann, 1994)). Since the industrial revolution in the 18th century, humans have emitted huge amounts of greenhouse gases, especially CO2 (from 275ppm in 1750 to 390 ppm today (IPCC, 2007)). By our extensive use of fossil fuel, cement production, biomass burning and deforestation it is "very likely"[12] that humans are responsible for the climate warming.

The multiple consequences and feedback mechanisms of a rising global temperature are complex and difficult to predict. In this study we focus on precipitation changes, and the IPCC Forth Assessment Report (2007) states that with a future warmer climate, precipitation generally seems to increase over the tropics and high latitudes and decrease over the subtropics. Southern Africa is already experiencing a temperature rise, expected to be of 3-4 ° C within this century (Christensen et al., 2007). The climate models are disagreeing more when it comes to precipitation predictions over southern Africa. Similarly are the historical meteorological records highly variable with no distinct patterns of changes in the rainfall amount, though the frequency and intensity of extreme events seems to be increasing(Christensen et al., 2007).

Though uncertain, most GCMs and RCMs agree that the south-western parts of southern Africa become drier, with a reduction in both intensity and number of rainy days. In contrast, the equatorial parts and the north-eastern plateau is predicted to become wetter, with an increase in the total rainfall rate while the number of rain days remains the same, implying more intense and extreme rainfall (Engelbrecht et al., 2008; Tyson and Preston-Whyte, 2000; Hudson and Jones, 2002; Tadross et al., 2005; IPCC, 2007). The frequency of the warm ENSO phase might be strengthened as a result of climate change(UNEP, 2006).

## 2.3 Agriculture

As described above, southern Africa has a highly variable precipitation rate, both in timescale and distribution. How does this affect the southern African people in their everyday life, and what happens if the climate changes ?

[11] Not considering feedback-mechanisms
[12] Very likely is more than 90 % likely after IPCC

> Agricultural production and food security in many African countries and regions are likely to be severely compromised by climate change and climate variability (Boko et al., 2007) .

Agriculture is the mainstay in the southern African communities, employing 75 % of the population and accounting for about 25 % of the GPD (Jury, 2002). Through its impact on the water section and aggriculture, climate change is of key importance to the economic development in this region. Maize is the most produced and highest consumed cereal in southern Africa, covering 40% of the calories consumed in the diet.

Southern African farmers are divided into two groups; a small party of commercial farmers and a large group small scale land holders. The commercial farmers are producing the largest amounts and have better utilisation of the fields (5 tonnes maize per hecta[13] ) while the rest, being the great majority of farmers, use underdeveloped methods and produce 10% of what could possibly be retrain from their cultivated land (1 tonne per hectar, holding potentially 10 tonnes of maize per hectar (UNEP, 2006).

Maize is normally planted in October and November while harvest time is around April and May. The first stage of crop growth requires ample soil moisture. The transition to the generative stage (formation of flowers) often occurs around January and is particularly sensitive to drought stress. Since the 1970s the growth in maize production has been scarce, leaving over half of the population under the limit for food-insecurity. With a growing population, the insecure food situation is aggravated by factors like floods and droughts, pore soil, failed policies and defective support systems. From early 1980s until mid-1990 persisting dry conditions also caused an increased pressure on the scarce water resources (Mason and Jury, 1997).

Adaptation has always been a key factor in farming, and of particular interest the recent years, as the climate variability seems to get more extreme. Local communities in southern Africa try to decrease their risks by the use of mixed crops and varying the planting sites, but there is a need for a rapid and structured development of new technology. Regularity of rainfall is critical for crop growth. If climate change results in more irregular distribution including dry spells, crop losses can be severe despite of unchanged total rainfall. For perennial crops like banana the question is if there is enough available moisture for survival of the dry season[14].

Most of the countries require a guiding policy for the market to develop new crop and livestock products, for instance setting up irrigation installations or improving the infrastructure. Especially when it comes to water

[13] 1 hectar= 10000 $m^2$

[14] After private communication with Trygve Berg, hydrologist at Ås Landbrukshøyskole.

supplies, the majority of the countries in southern Africa have only developed a small share of their "'irrigation potentials"', where South Africa is a great exception (using 100% of the potential)(Svendsen et al., 2008).

Though adaption and mitigation are essential precautions, one have to keep in mind that the nature is powerful and humans can not be protected against everything. In occurrences of extreme events like severe droughts and floods, the adaptive efforts might be of little value in that specific region. Before 1970s, extreme events of floods and droughts happened on a time scale of 10 to 20 years, making the communities able to rise again in between each damaging incident. In recent years the frequency of extremes seems to be increasing, forcing the local farmers to sell their degraded land and migrate to cities(UNEP, 2006). Nevertheless, in an incident where some communities are severely damaged, they will be totally depended on the regions around. Thus, making the precautions for a changing climate can limit a potential catastrophe, and if extreme events strikes it is even more important that adjacent regions prepared for adaptation. High resolution information on future precipitation patterns can be essential in the process of making such adaptive strategies (UNEP, 2006; Jones and Thornton, 2003). A higher precision in precipitation intensity, duration and location will provide the local farmers with knowledge of when, where and what to plant. Hopefully, it will also give decision makers sufficient information to initiate mitigation processes.

# Chapter 3

# Model and methodology

**Regional climate modeling**

Regional climate modeling is becoming increasingly popular, aiming for higher resolution information than what a global climate model can provide. As mentioned, a RCM is usually initialized by time-depended driving fields from a GCM on the lateral boundaries, SSTs and land-surface conditions. The main idea is that the driving GCMs will provide large scale circulations, and the RCM will resolve the meso-scale processes and by including physical schemes, also solve the microphysical processes. When using this technique, some issues are important to have in mind:

- Any errors from the forcing data (GCMs or SSTs) will to some extent be carried through, but might be counterbalanced by the physical parametrization in the RCMs.
- The location and size of the domain is essential. The domain should be large enough so that internal circulations can develop, without the possibility of deviating too much from the GCM input.
- Representation of the physical and dynamical processes today, is assumed to hold for the future.

(Tummon, 2011; Giorgi et al., 1994; Sylla et al., 2011)

## 3.1 The WRF model

WRF is a mesoscale numerical weather forecasting-model that serves both for operational forecasting as well as research. The model consists of several components working together. There are two main elements in WRF:

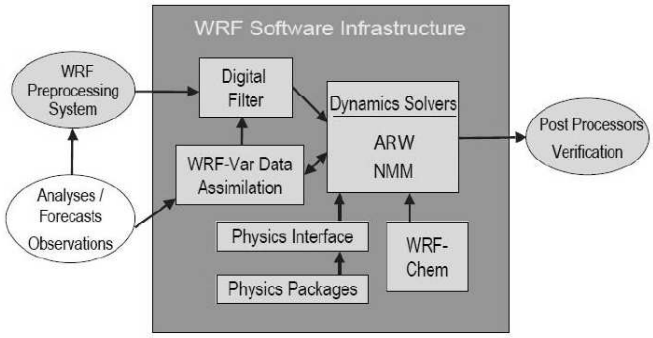


**Figure 3.1:** *WRF components and data flow*

- The WRF Pre-Processing System (WPS): WPS prepares meteorological and geographical input for WRF.

- The dynamic solvers: There are two dynamic solvers in WRF. The Advanced Research WRF (ARW) is mostly used for research and the Nonhydrostatic Mesoscale Model (NMM) is utilised for operational forecasting.

Several packages, such as physical parametrization schemes, WRF-Chem and WRF-VAR, are compatible with WRF (Figure 3.1).

WRF is a result of a multiagency collaboration, consisting mostly of the National Center for Atmospheric Research (NCAR), the National Centers for Environmental Prediction (NCEP), the Forecast Systems Laboratory (FSL), the Air Force Weather Agency (AFWA), the Naval Research Laboratory (NRL), Oklahoma University, and the Federal Aviation Administration (FAA). The model is updated each year( sometimes even few times a year) and new versions made public. The version used in this thesis is WRFV3.2.

## 3.2 ARW - the dynamic solver

In this study, the Advanced Research WRF (ARW) has been used as the dynamic solver of the governing equations of atmospheric dynamics. It solves the non-hydrostatic Eulerian equations by using a time-split third-order Runge-Kutta scheme (RK3). The vertical coordinate in WRF is a terrain-following hydrostatic pressure coordinate $\eta$ (see Figure 3.2), which introduces a set of equations for the compressible non hydrostatic equations. The coordinate is defined as

$$\eta = \frac{p_h - p_{ht}}{\mu} \tag{3.1}$$

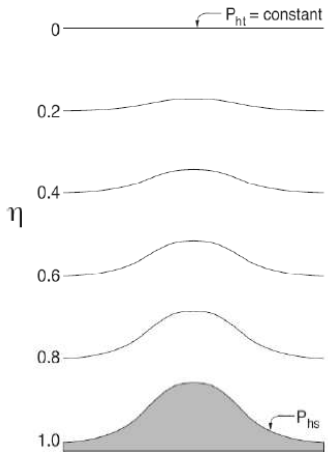


**Figure 3.2:** *$\eta$ -levels in ARW*

Where $\mu = p_{hs} - p_{ht}$ and $p_h$ represents the hydrostatic component of the pressure, on the surface ($p_{hs}$) and on the top boundary ($p_{ht}$). $\mu(x, y)$ expresses the column mass of dry air per unit area at (x,y), thus the variables for the flux form equations ((3.3)-(3.8)) can be defined as

$$\vec{V} = \mu\vec{v} = (U, V, W), \quad \Omega = \mu\dot{\eta}, \quad \Theta = \mu\theta, \tag{3.2}$$

$\vec{v} = (u, v, w)$ are the horizontal and vertical covariant velocities, while $\omega = \dot{\eta}$ represents the contravariant vertical velocity. $\theta$ express the potential temperature. With these definitions, six prognostic Eulerian equations can be defined on flux form; three momentum equations, the thermodynamic equation, the continuity equation and the material derivative of the geopotential

$$\partial_t U + (\nabla \cdot \vec{V}u) - \partial_x(p\phi_\eta) + \partial_\eta(p\phi_x) = F_U \tag{3.3}$$

$$\partial_t V + (\nabla \cdot \vec{V}v) - \partial_y(p\phi_\eta) + \partial_\eta(p\phi_y) = F_V \tag{3.4}$$

$$\partial_t W + (\nabla \cdot \vec{V}w) - g(\partial_\eta p - \mu) = F_W \tag{3.5}$$

$$\partial_t \Theta + (\nabla \cdot \vec{V}\theta) = F_\Theta \tag{3.6}$$

$$\partial_t \mu + (\nabla \cdot \vec{V}) = 0 \tag{3.7}$$

$$\partial_t \phi + \mu^{-1}[(\vec{V} \cdot \nabla\phi) - gW] = 0 \tag{3.8}$$

The right-hand-side of equations (3.3) - (3.6) represent the forcing terms ($F_\Theta$, $F_U$, $F_V$ and $F_W$). $\phi$ is the geopotential and p expresses pressure. The diagnostic relation for the inverse density, $\alpha = 1/\rho$, can be written as

$$\partial_n \phi = -\alpha\mu, \tag{3.9}$$

along with the equation of state

$$p = p_0 \left( \frac{R_d \theta}{p_0 \alpha} \right)^{\gamma} \tag{3.10}$$

where $\gamma = c_p/c_v = 1.4$ is the ratio of heat capacity for dry air, $R_d$ represents the gas constant and $p_0$ a reference pressure.

In equations (3.3) - (3.8) the subscripts $x$, $y$ and $\eta$ denote differentiations

$$\nabla \cdot \vec{V}a = \partial_x(Ua) + \partial_y(Va) + \partial_\eta(\Omega a), \tag{3.11}$$

and

$$\vec{V} \cdot \nabla a = U\partial_x a + V\partial_y a + \Omega\partial_\eta a, \tag{3.12}$$

where $a$ represent a generic variable.

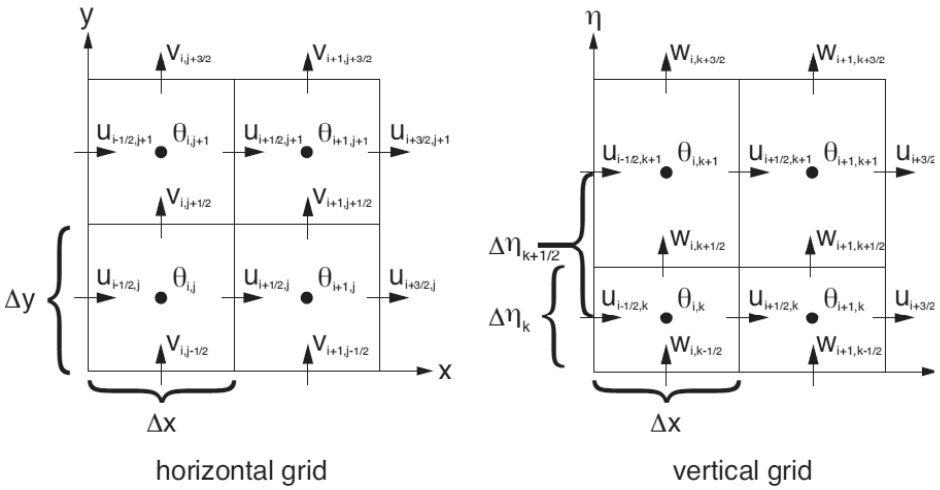


**Figure 3.3:** *Arakawa C grid staggering in the horizontal and vertical (Skamarock et al., 2007)*

The equations can not be solved analytically, thus a discretization method is needed. The atmosphere is divided into grid boxes and the complex equations solved for each box. ARW use Arakawa C grid staggering shown in figure 3.3. The $(i,j)$ points are defined in the middle of the grid boxes, and the thermodynamic variables ($\theta$) are calculated here. The velocities $(u, v, w)$ are staggered one half grid length from $(i,j)$, defined on the edges of the grid-boxes, for easier calculation of the advection in and out of the grid.

As mentioned, the ARW uses a third-order Runge-Kutta (RK3) time integration scheme on meteorologically significant modes, but high frequency acoustic modes are integrated over smaller time step to maintain numerical stability (Skamarock et al., 2007; Skamarock and Klemp, 2008). To make

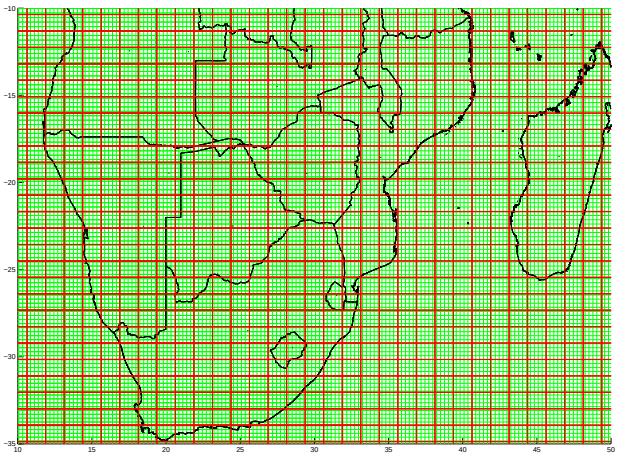


**Figure 3.4:** *Domain over southern Africa. WRF grids (green) and CAM grids (red)*

sure that RK3 is stable, it is recommended in the users guide to set the time step (in seconds) less or as large as 6 times the resolution of the domain (in km). This is a separate choice that can be specified in the namelist. [1]

## 3.3 Model setup

Previous studies have noted that whether Madagascar is included in the domain or not could be of importans for the circulation patterns over southern Africa[2](Landman et al., 2005; Tummon, 2011). A testrun without Madagascar resulted in enormous overestimation of precipitation along the eastern coast of Africa. Thus, the final domain in this study includes Madagascar, and stretches from 5° to 38° S and 8 ° to 53° E, with a resolution of 27km x 27km (figure 3.4). This results in a model domain containing 175 boxes in east-west direction and 139 boxes in the north-south direction. The number of vertical layers has been chosen as a trade-off between simulations speed and quality of results. Based on previous studies and recommendations, the final runs contains 36 vertical layers (top boundary ($p_{ht}$) = 10hPa). The time-step in WRF is 160 seconds.

### 3.3.1 Initialisation and boundary condition

WRF is initialised and driven by input data extracted from CAM4. CAM4 is a global atmospheric model from NCAR used for weather and climate

[1]More about the discretization method and time step choices can be found in Wicker and Shamarock 2002.

[2]See circulations in Figure 2.7

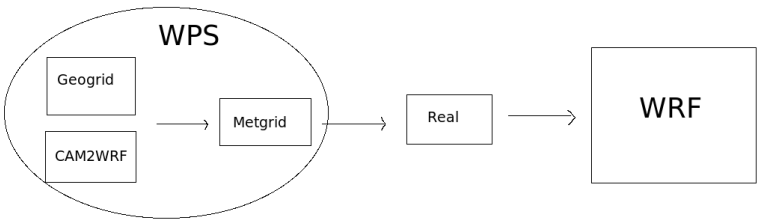


**Figure 3.5:** *The setup used in this study to produce input files for WRF.*

research. For this study, CAM has run in a transient mode with prescribed SSTs, GHGs, aerosols and ozone. The input data from CAM have a resolution of 0.9 $^0$ x 1.25 $^{0\ 3}$. The land-surface boundary conditions (soil moisture and temperature) in WRF has been initialised by CLM[4] datasets.

CAM is forced with varying SSTs, thus for consistency WRF is forced by the same dataset. For the first time slice (1990-2009), we have used observed SSTs from HAdISST [5]. For the future scenario , outputs from the Parallel Ocean Program (POP) model[6] are employed. WRF is forced by extracted CAM variables (see section 3.4)at the lateral boundaries in addition to SSTs every 6 hours.

### 3.3.2 The WRF Pre-Processing System (WPS)

CAM, CLM and SST data are prepared for input to WRF by the WPS, which contains three main programs; geogrid, ungrib and metgrid. The WPS defines the domain, interpolate static geographical data to the grids, extracts the initial meteorological fields needed from GRIB files and interpolate them to the model grids. In this study, geogrid is run with geographical data downloaded from `http://www.mmm.ucar.edu/wrf/src/wps\_files/` , which has a resolution of less then 1km.

The input data from CAM, CLM and SSTs are not GRIB files (netCDF). Thus extracting the initial meteorological variables to the right intermediate-formate for input to metgrid (normally computed by ungrib) is in this study performed outside of the WPS by a separate program called CAM-to-WRF[7] (see Figure 3.5). With some modifications on geogrid and metgrid,

[3]CAM is run with 26 vertical layers, a time step of 1800 seconds and outputting averaged data every month.

[4]Community Land Model (CLM) is the land model in CCSM.

[5]HadISST is a monthly long-term global sea surface temperature (SST) and sea ice analysis with one-degree resolution from The Met Office Hadley Center.

[6]POP is a part of NCAR's Community Climate System Model(CCSM).

[7]Performed by Sandeep Sukumaran working for the SoCoCa-project.

the WPS makes the right input data for WRF. Hence, the input data has been interpolated to the pressure levels ($\eta$-levels), soil levels (0-10cm and 10-200cm) and map-projection (Mercator) used in WRF. The vertical coordinates in CAM (hybrid) is transformed to WRF's $\eta$-levels.

### 3.3.3 The physical schemes in WRF

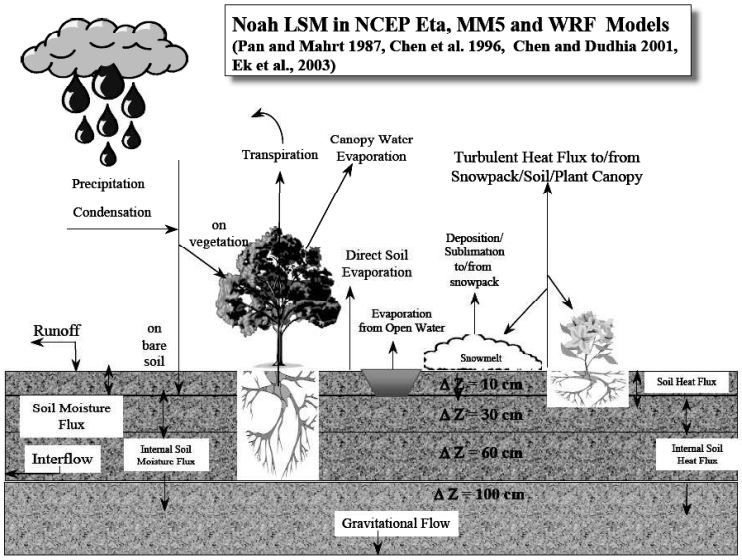


**Figure 3.6:** *Noah land surface model used in this study*

WRF offers a wide range of schemes representing various physical and dynamical processes. These can be combined in many ways, and are all varying in complexity and computational time (see Table 3.0). The best combination of schemes depends on the placement, size and resolution of the domain and the processes in focus. There are previous studies exploring the combinations of different schemes for specific events (Flaounas et al., 2010; Venkata et al.; Gochis et al., 2002; Cretat et al., 2011), however none of these are long term simulations with high resolution over southern Africa. As each simulations seems to be quite unique for the different WRF parametrization, it is recommended to run various options and compare the results to find the best combination (Flaounas et al., 2010). The ARW User Guide gives recommendations for scheme choices in regional climate modeling (Wang et al., 2007), but it is important to have in mind that this is just guide lines, as all regions require different combinations. Sensitivity studies were not performed in advance of computing the longer runs in this study [8]. The scheme options were chosen as a compromise based on recent and ongoing studies, recommendations from the ARW User Guide, restrains in WRF for combinations of schemes and computational efficiency.

[8] As mentioned in Chapter 1, sensitivity studies were not performed in advance of the study because of time-limitations.

| | |
|---|---|
| Shortwave Radiation | Dudhia (MM5)<br>Goddard<br>CAM<br>GFDL |
| Longwave Radiation | RRTM<br>CAM<br>GFDL |
| Surface Layer/Boundary Layer | Yonsei University PBL<br>Mellow-Yamada-Janjic PBL<br>ACM2 PBL<br>MRF PBL |
| Land Surface | 5-layer Thermal Diffusion<br>Noah LSM<br>RUC LSM<br>Pleim-Xiu LSM |
| Cumulus Parameterization | Kain-Fritsch (new and old versions)<br>Betts-Miller-Janjic<br>Grell-Devenyi<br>Grell-3 |
| Microphysics | Kessler<br>Lin et al.<br>WRF Single Moment (WSM3, WSM5, WSM6)<br>Eta (Ferrier)<br>Thompson<br>Goddard<br>Morrison 2-moment |

Table *3.0. Different physical scheme alternatives in WRF, representing various physical processes (UCAR-edu, 2008)*

The physical processes and their following scheme options used in this study, are listed in Table 3.1. The Planetary Boundary Layer scheme (PBL), the Land Surface Model Scheme(LSM) and the cumulus parametrization scheme can all be of significant importance in the process of convective precipitation. The PBL scheme chosen for this study is Yonsei University scheme (YSU): a non-local-K scheme with explicit entrainment layer and parabolic K profile in unstable mixed layer. The land surface model Noah[9] predicts both soil temperature and moisture. YSU and Noah are advised in the WRF Users Guide to utilise in a regional climate run for resolution less than 30km (Bukovsky and Karoly, 2009).

Kain-Fitsch scheme represents the cumulus parametrization, and is a low-level convective scheme where activation of convection is based upon low-level forcing. A parcel must be lifted to the level of free convection to onset deep convection. Once the convection is onset, the scheme consumes the entire CAPE[10] in a 50-100hPa thick trigger layer, during a convective

[9]Noah is an abbreviation for the developers of this LSM. N: National Centers for Environmental Prediction (NCEP), O: Oregon State University (Dept of Atmospheric Sciences), A: Air Force (both AFWA and AFRL), H: Hydrologic Research Lab).

[10]CAPE stands for Convective Available Potential Energy.

| | |
|---|---|
| Shortwave Radiation | CAM |
| Longwave Radiation | CAM |
| Surface Layer / Boundary Layer | YSU |
| Land Surface Model | Noah |
| Cumulus Parametrization | Kain-Fritsch |
| Microphysics | Lin et. al |

**Table 3.1:** *Scheme chosen for this study.*

cycle of 30-60 minutes (UCAR-edu, 2010). According to ongoing studies, this scheme can reproduce the amount of heaviest precipitation more accurately than other schemes and perform relatively well compared to other schemes in Africa (Mesquita et al., 2010; Fernandez, 2010). Kain-Fritsch is also recommended by the ARW User Guide for regional climate runs(Wang et al., 2007).

CAM radiation schemes allow for updating greenhouse gases. Thus, in this study the radiation schemes have been modified to update greenhouse gases every year. The concentrations of gases are taken from the driving global climate model (CAM) following RCP4.5 (see appendix A), which are linearly interpolated for every time-step value(Fita et al., 2010).

### 3.3.4 Other scheme choices

Two different scheme options, Grell cumulus scheme and MYJ PBL scheme, have been tested in additional shorter sensitivity runs (computed after the historical run, further explained in Section 4.3/4.5). The 2002 version of Grell cumulus scheme applied here (Grell and Devenji) is based on a simple type of Arakawa-Scubert scheme, a one-dimensional mass flux scheme consisting of a single updraft-downdraft couplet. The scheme uses an ensemble mean (of 144 ensembles) with several alternatives of closure and changes of the sensitivity parameters[11]. MYJ (Mellor-Yamada-Janjic scheme) Eta operational scheme is a one-dimensional prognostic turbulent kinetic energy scheme with local vertical mixing, based on Turbulent Kinetic Energy (TKE).

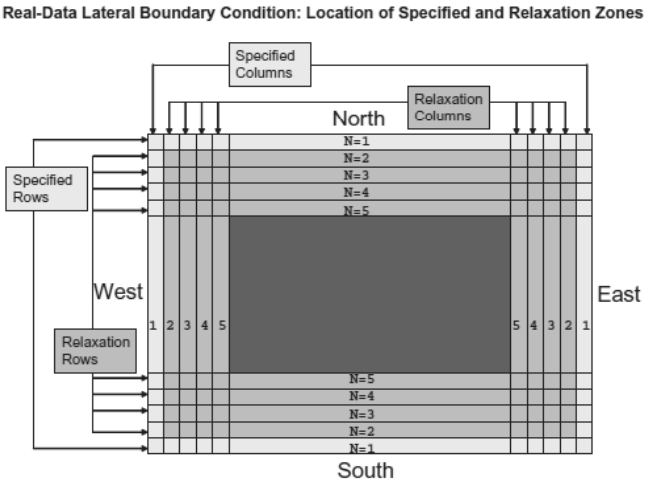


**Figure 3.7:** *Lateral Boundary Condition: Specified and relaxation zones (Skamarock et al., 2007)*

## 3.4 Computational description and modifications

WRF is originally used as a forecasting model with outputs of instantaneous values, except for rainfall. Thus, the source code has been modified and additional parts have been added, to calculate daily maximum, minimum and average values of surface temperature, horizontal winds and humidity[12]. This was performed with technical help through mail correspondence with the Santander Meteorology Group. (Fita et al., 2010). For WRF to update SSTs, it needs to be specified and computed as a separate inputfile for WRF. Seasonal changes of the background surface albedo and vegetation fraction has also been added. As mentioned in the previous section, the radiations schemes (CAM short and longwave) have been modified to update greenhouse gases every year.

Additional modifications were needed to run WRF for climate applications, to avoid small scale systems to grow and become unstable or generally just diverge too much from the forcing fields. As illustraded in figure 3.7, WRF operates with a specified lateral boundary zone, containing an outer "specified column" and inner "relaxation columns". The specified column is determined entirely by the interpolation of the CAM forcing, while in the relaxation zone the model is forced towards the input data only to a certain degree. To allow enough freedom for the model to develop its own internal circulation, regional climate modelers prefers to avoid internal nudging.

[11]Four different types of closure (e.g removal of CAPE (Kain Fritsch as used originally), moisture convergence (Krishnamurti et al 1993), quasi equilibrium (Arakawa and Schubert 1974) and low-level vertical velocity (Brown 1979)) are adopted and in combination with changes in parameters such as entrainment, could-radius, precipitation efficiency and other.)

[12]Variables also specially chosen to of value for hydrologists at the SoCoCa-project.

Instead, it is common to force the model strongly towards the driving fields in a large relaxation zone. In this study we have therefor enlarged the relaxation zone from the default of five grid points to ten grid points and changed the nudging coefficient from linear to exponential (Wang et al., 2007). According to Girogi 1999, this method results in a smoother transition than the linear relaxation scheme and provides a better transition from the boundary to the model interior.

**Technical steps**

The CAM data has been written to intermediate format for input to WRF, by modifying the source code following the ARW Users Guide[13]. Temperature, relative humidity, horizontal winds and geopotential height (all 3D fields), sea level pressure and surface pressure (2D fields) are given as input to WPS (and thus WRF).

The 20 year run has been simulated through 6 smaller runs using restart files. As mentioned, there are three main steps to perform when dynamically downscaling with WRF (see Figure 3.5): WPS (described shortly in above Section 3.3), Real (which makes the initial and lateral boundary files) and WRF itself. As storage space has been an issue, each of the 6 smaller runs have to go through all steps, finish and be moved to an external saving account, before running the next part. Back and forth moving of the data has been very time-consuming.

The runs are computed on a supercomputer at the University of Oslo (TITAN[14]), running at the maximum on 80 parallel nodes. In this study, WRF gives output every month (containing daily values) varying around 2.2GB in size. For post-processing of the data (averaging, merging of files etc.), nco and cdo- commands have been used. The netCDF output from WRF is not fully align with the common netCDF convention, thus a script from the University of Bergen [15] has been run, after interpolating the output files to pressure levels by an additional post-processing script (p_interp[16]).

Matlab and ncl have been utilised for visualisation of the results.

There is an additional complexity of this study with the time-constraint of a master thesis, computational-limitations and saving space-issues, in

[13]The majority of this work has performed by Sandeep Sukumaran, following the steps from the Users Guide :`http://www.mmm.ucar.edu/wrf/users/docs/user_guide/users_guide_chap3.html\#_Writing_Meteorological_Data`.

[14]More information on TITAN can be found in `http://www.notur.no/hardware/titan/`

[15]Script for full netCDF conversion is provided by Torleif Markussen Lunde after mail correspondence.

[16]p_interp is provided by The Santander Meterology group in Spain.

addition to TITAN's unstable nodes (crashing and downtime). The main goal was to finish a historical 20 year run, entailing to start this run quite early in the study. Although we could see during this work that additional changes might benefit the outcome, these changes will rather be recommended for future work.

.

# Chapter 4

# Results

In this chapter, results from the regional climate model (WRF) run are presented. This thesis is a first attempt to downscale CAM by the use of WRF in southern Africa. Therefore aiming for a 20 year historical run and a 20 year future run was a very ambitious initial goal. As it occurred to be errors concerning the landmask in the 2050-2069 input data from CAM (see section 4.5), time constrains limited the study to leave the 2050-2069 run to future research. Thus, the primary focus of this study is how WRF reproduces the precipitation patterns in southern Africa and mainly results from the historical run (1990-2009) are presented and discussed. Nevertheless, a few preliminary results from a future testrun (2050-2069) are also shown.

It is of interest to consider WRF's performance by looking at different aspects of precipitation patterns (daily, seasonal, annual, interannual and extreme), related meteorological variables and possibly link the results to the chosen physical schemes. As a comprehensive and detailed analysis like this can not be carried out within the time horizon of a master thesis, the variables illustrated here will be qualitatively analysed and selected areas discussed. An important part of this work is also to give recommendations for further studies. These will be summarised at the end of this chapter.

In the following an overview of related meteorological variables (temperature, wind and pressure) in WRF will be given, by seasonal means (summer and winter). Then, the precipitation results from WRF are presented, and WRF and CAM simulations of precipitation are compared with observation data[1] for a validation. Next, the domain is divided into nine regions of focus, and the annual cycle of WRF, CAM and observational precipitation are presented by long term monthly means. A short description of the precipitation changes within 1998-2009 are also made. In addition, smaller testruns for different WRF setups are shown and discussed to gain more information on the chosen physical parametrization and possible alternatives

[1] A description of these data is given in the next section. Although these are mostly satellite data combined with observed data, they will for simplicity be called observed data throughout this thesis.

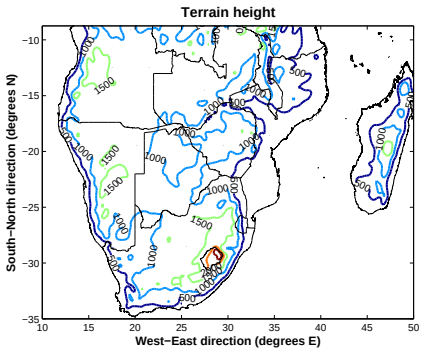


**Figure 4.1:** *Terrain heights (m.s.l) for the domain of focus, output from WRF*

for future runs. Finally, the testrun for the future simulation is presented and future work is suggested.

### General description of the presented data

The southern African continent is of main focus in this study, and the results over Madagascar will not be discussed[2]. The relaxation zone is not included in the plots or analysis, leaving an inner domain from 8° to 35° S and 11 ° to 50° E.

The results have mainly been evaluated by two different types of dataset. For long term seasonal and monthly precipitation, Global Precipitation Climatology Project (GPCP) Version-2 has been compared with WRF and CAM. GPCP consists of global, monthly analysis of surface precipitation at 2.5 ° x 2.5° resolution and is available from January 1979 to September 2009(Huffmana and Bolvin, 2009). The GPCP rainfall estimates are a combination of four independent satellite products (SMM/I emission, SMM/I scattering, GPI and OPI geostationary estimates and TOVS) and ground based rain gauge measurements. Monthly error estimate fields in GPCP are also calculated and downloadable[3]. The error fields have an absolute monthly mean maximum of 2 mm/day in the tropical parts, northeastern Mozambique and Mozambique Channel during summer. To evaluate the related meteorological variables, monthly means for 1991-2008 from a cooperative institute of the National Oceanic and Atmospheric Administration (NOAA) and the University of Colorado Boulder (NOAA-CIRES) have been used(Compo et al., 2006). The dataset has a resolution of 2 ° x 2 ° and is

[2]As outlined in Chapter 3, Madagascar is included for better representation of the circulation over southern Africa. An analysis of Madagascar would demand an even larger domain.

[3]With GPCP Version 2.1 Combined Precipitation Dataset one can also retrieve estimates of random error (The random error depends on sensor quality, number of samples, and precipitation rate, more information of the calculations methods can be found in Adler et al. (2003).

obtained from Physical Climate Division (PSD) Gridded Climate Datasets [4]. It should be noted that the satellite observational datasets are of coarser resolution than WRF. Thus some of the local effects resolved by WRF will not be evident in the observed data, and one could question whether local deviations arise from model error or as a cause of better resolution. Local level biases should be analysed with this in mind.

The monthly and seasonal means of the datasets have been computed by arithmetic averaging.

$$A = \frac{1}{n} \sum_{i=0}^{n} a_i \tag{4.1}$$

For regional climate applications of WRF, a larger spin up time is recommended (Wang et al., 2007). To ensure that the landsurface model has spun adequately, this study requires a spin up time of at least a couple of months[5]. For consistency in time when comparing monthly, season and annual plots, we have therefor disregarded the first simulated year[6]. Additionally GPCP and NOAA are only downloadable for up until 2008, the main results presented here are for the time period of 1991-2008.

Throughout this chapter, results from CAM are shown to provide further information of how WRF performs as a dynamical downscaler. Thus, the CAM results will mostly be addressed when assessing valuable information compared to WRF. The datasets obtained from CAM, WRF, GPCP or NOAA-CIRES will mostly in the following sections only be referred to the models/datasets names (CAM, WRF, GPCP and NOAA-CIRES) for simplicity.

## 4.1 Long term seasonal means for 1991-2008

To get an overview of WRF's ability to reproduce the general climate over the 1991-2008, seasonal climatologies from the simulations (WRF and CAM) and observed data (GPCP) are presented and compared in this section. It has been stressed during this study to run WRF for a long time period, to compute such climatologies with less influence from specific extreme incidents. Although this amount of data demands huge storage space and is computationally heavy, it provides a better platform to look at the performance of WRF as a regional climate model.

Austral summer climatologies are computed by averaging over December, January and February, hereafter denoted as DJF. Austral winter climato-

[4]Downloaded from their Web site at http://www.esrl.noaa.gov/psd/

[5]Recommendation after private communication with Cindy Bruyere, scientist at UCAR.

[6]December 1990 and 2050 are included in the seasonal average for the austral summer season.

logies are averages over June, July and August, from now on denoted as JJA.

### 4.1.1 Precipitation related meteorological variables: wind, temperature and geopotential height

WRF averages a few selected variables (10m wind, 2m temperature, 2m moisture, skin temperature and precipitation) at every second minute while running, after additions to the source code were made for this study. The rest of the outputted variables are daily instantaneous values taken at 00:00 UTC[7]. Means of diurnal varying variables would in itself have discrepancy when comparing observed values with WRF (means of 00:00 UTC) and are of less value analysing.

Geopotential heights (at 1000hPa, 850 hPa and 500 hPa), 2m temperature and 10m wind are presented here. The variables are included to provide further information concerning the precipitation patterns, and features with potential direct affect on the rainfall rate will be pointed out and qualitatively studied. CAM outputs contains averages of temperatures at 2m, while the other variables use pressure heights as vertical level of reference (which WRF only can provide for means of variables at 00:00 UTC), thus 2m wind from WRF will only be compared to observed data.

Geopotential heights from WRF, CAM and NOAA-CIRES are compared in Figure 4.2 and Figure 4.3, for winter and summer climatologies respectively. The geopotentials in WRF are computed over means of instantaneous outputs at 00:00 UTC [8]. Figure 4.2 shows that the general patterns of the geopotential heights at 1000hPa are reproduced by WRF, but both models simulate a deeper than observed Angola low. By 850hPa the differences are less, and the minimum (center of the cyclone) is actually higher in WRF than in GPCP. At 500hPa, the geopotetnial heights are situated quite equally, only somewhat higher in WRF. This means that WRF has a larger $\Delta\Theta_{500hPa-1000hPa}$ than what is observed, indicating a column of higher mean temperature (latent heat) in WRF than what it seen in GPCP.

The winter Kalahari high is reproduced in the models (Figure 4.3), but the geopotential heights are overestimated, especially at 1000hPa. Notice that the Kalahari high pressure seems to extend into the South Indian High pressure, and lies further south than observed. Thus the midlatitude anticyclone is displaced south in WRF with respect to NOAA-CIRES.

[7]Saving space and computational resources limited the output to one each day in this study.

[8]The diurnal variation is small regarding geopotenitals for synoptic cyclones and anticyclones that are present in the seasonal climatologies made here.

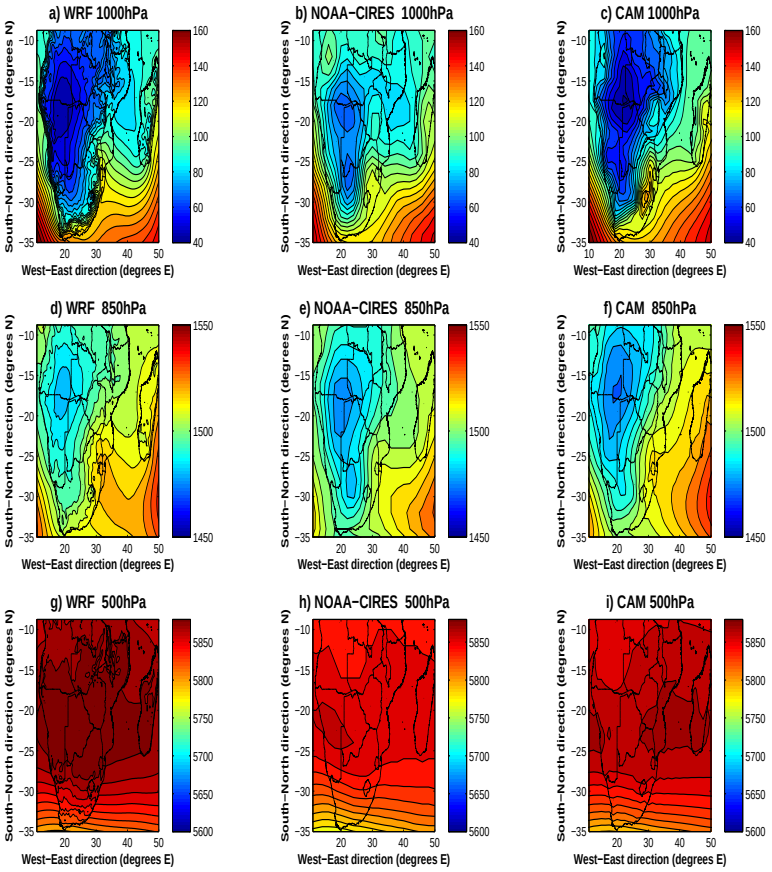


**Figure 4.2:** *Seasonal average for WRF, CAM and NOAA-CIRES of geopotential heights (m) over the summer months DJF, for 1000 hPa (a-c), 850 hPa (d-f) and 500 hPa (g-i)*

In Figure 4.4 DJF and JJA 2m temperature means from WRF, CAM and NOAA-CIRES are plotted. All three figures show similar patterns. For both DJF and JJA, WRF seems to underestimate the temperature over most of the continent, particularly at higher altitudes (Blackenberg mountain range in the southeast). The land-sea surface temperature contrast is larger in WRF than in CAM along the southeastern coast, where the (Figure 4.4 b,d,f). Generally, the CAM simulations of surface temperatures have less bias and are quite successfully reproducing the temperatures in JJA (this could be an effect of more similar resolutions).

WRF slightly overestimates the temperature on the northern border of Zimbabwe and around lake Malawi in DJF. Relatively higher temperatures are also spotted over Lake Malawi for WRF in winter season. The differences over Lake Malawi draws special attention, as this study does not include any coupling to lake models. WRF simply chooses the closest

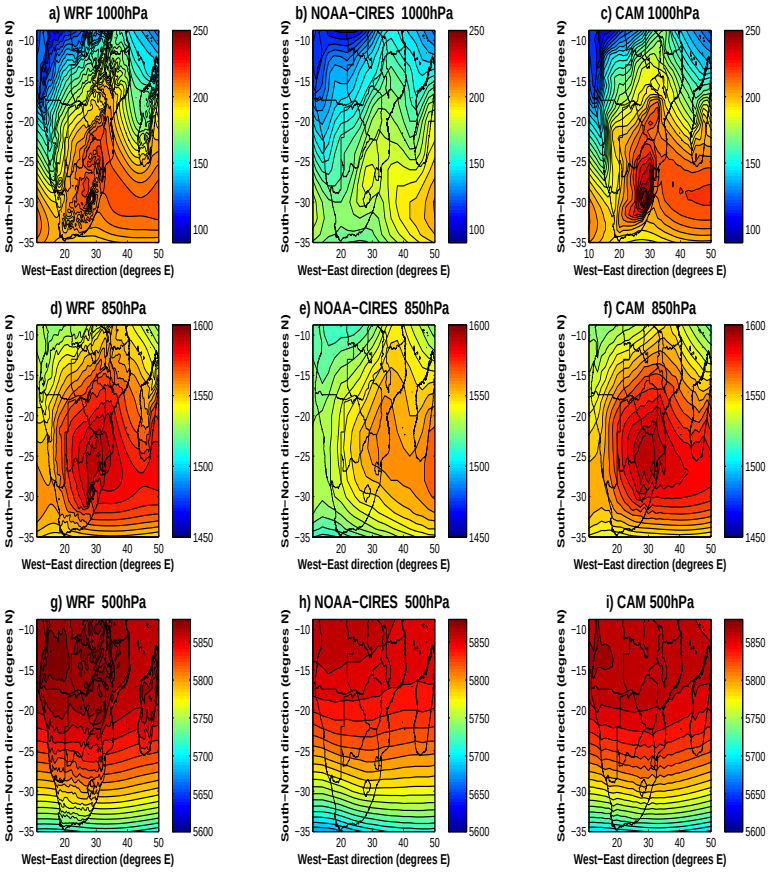


**Figure 4.3:** *Seasonal average for WRF, CAM and NOAA-CIRES of geopotential heights (m) over the winter months JJA, for 1000 hPa(a-c), 850 hPa (d-f) and 500 hPa (g-i).*

SST values for skin temperatures in lakes, which in this case is the SSTs in the Mozambique Channel. The temperatures have not been changes as they seems to range within a reasonable values compared to measured temperatures found in previous studies[9]. However, the temperatures might differ from observed on a temporal scale, and as this could be a source of error the results around Lake Malawi should be analysed with care. The deviations from observations over local areas in WRF, could be a direct effect of the coarser resolution in NOAA-CIRES, meaning that 2 °x 2 °resolution is not high enough for capturing the temperature changes in these areas (e.g Malawi and Blackenberg).

Surface wind patterns (10m) from WRF are well captured, especially for DJF. As one can see from Figure 4.5a, the convergence zone and the southern ITCZ lies around 17 $^0$ S in both WRF and NOAA-CIRES. The cyclonic

[9]In WRF the skin temperature ranges from 24 to 28 degrees, as found to be the same as measured temperatures : http://www.aslo.org/lo/toc/vol_50/issue_2/0727.pdf.

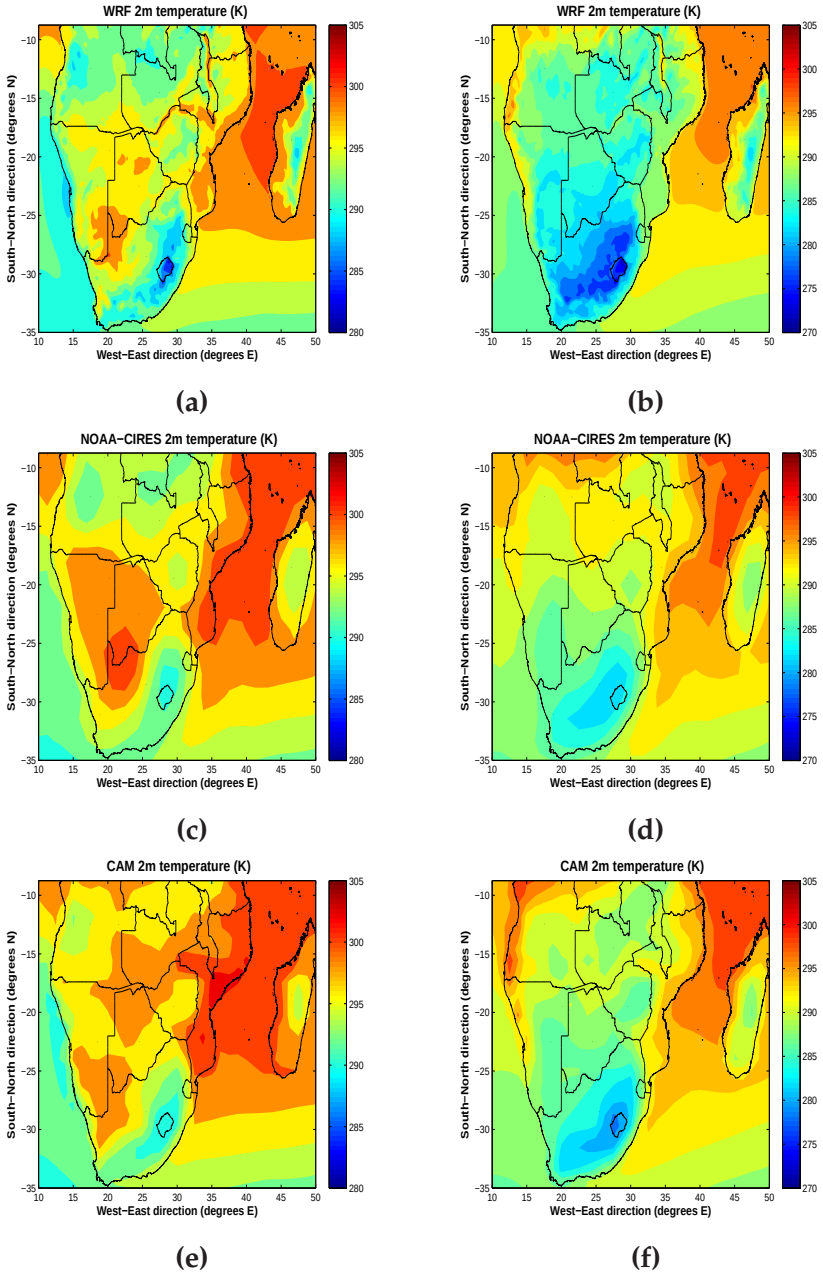


**Figure 4.4:** *Climatology of 2m temperature (Kelvin) for winter (JJA) and summer (DJF) season. a) WRF (DJF), b) WRF (JJA), c) NOAA-CIRES(DJF), d) NOAA-CIRES (JJA), e) CAM (DJF) f)CAM (JJA). Notice different temperature interval for DJF and JJA.*

circulation (Angola easterly low) is situated right at the boarder of Angola and Namibia. WRF generally overestimates the strength of the wind in the oceans and slightly over land areas in JJA , while the strength is somewhat less than observed on the southwestern coast in DJF. Additionaly, in JJA the south westerlies (assuming the 10m wind is representative)i n WRF are stretching slightly less northwards than in NOAA-CIRES, which could be linked to the stronger and southwardly displaced Kalahari high pressure

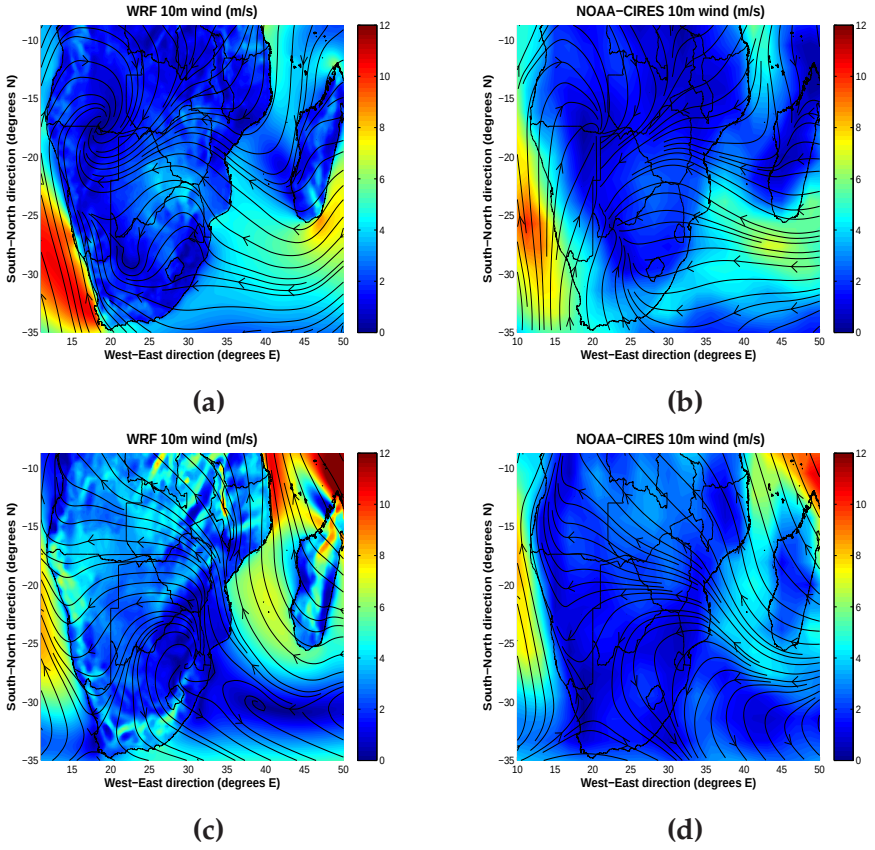


**Figure 4.5:** *Seasonal average of 10m surface winds(m/s) over DJF and JJA: a) WRF (DJF) b) NOAA-CIRES (DJF) c) WRF (JJA) d) NOAA-CIRES (JJA). Be aware that the density difference in the wind trajectories between WRF and NOAA-CIRES, only arise from resolution difference, and is not a measure of wind strength. Look only at the colors for windstrength.*

seen WRF (see Figure 4.3b and 4.3e and Section 4.1.1).

Focusing on Lake Malawi, there is an abrupt wind change which is not captured in NOAA-CIRES. This could, as seen for the temperatures, either indicate erroneously representation of winds over Lake Malawi in WRF, or that the area holding abrupt wind change is too small to be resolved in NOAA-CIRES.

A more detailed analysis in the vertical or verification of other variables falls beyond the time-horizon of this thesis.

### 4.1.2 Precipitation in WRF and CAM vs. GPCP

In this section the seasonal precipitation in WRF is presented. The mean winter and summer season of precipitation in WRF and GPCP are shown for an overview. Then the deviations from WRF and CAM with respect to

GPCP are presented and discussed.

Summer and winter precipitation climatologies in WRF and GPCP can be seen in Figure 4.6. As discussed in the Chapter 2, most of the precipitation over southern Africa is received on the northeastern side of the plateau, with the heaviest rainfall rate during DJF. In JJA it is generally dry on the south African plateau, with the exception from the southern tip receiving its yearly rainfall at this time. Figure 4.6 indicates that WRF quite successfully reproduces the seasonal cycle of precipitation. The climatological division between the wet northeast and dry southwest is clearly evident.

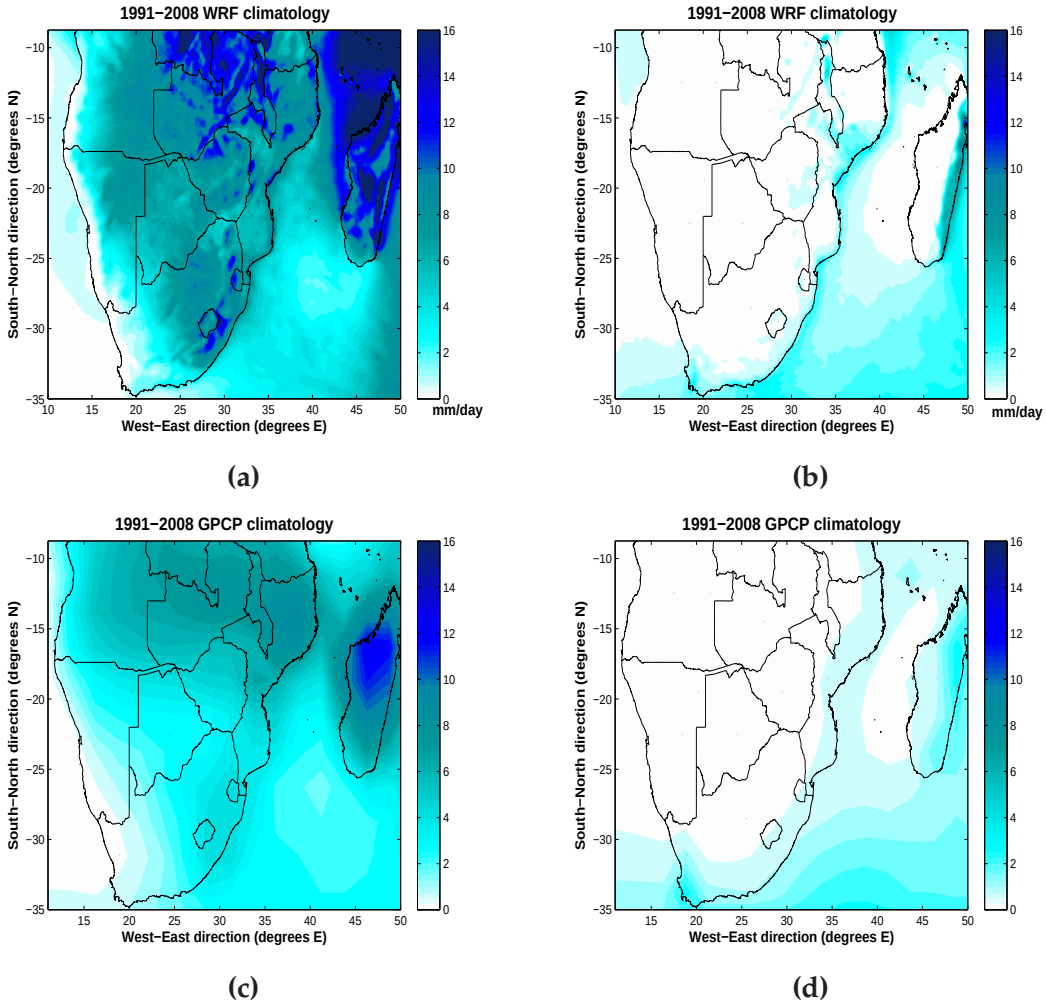


**Figure 4.6:** *Seasonal climatology of precipitation (mm/day) for WRF for a) summer (DJF) and b) winter (JJA) and observed GPCP c) summer (DJF) and d) winter (JJA).*

To closer evaluate the seasonal climatologies of precipitation in WRF, the results are compared to data based on GPCP on a grid scale. Thus WRF and CAM precipitation has been area averaged to the larger grids in GPCP (2.5°x 2.5°).

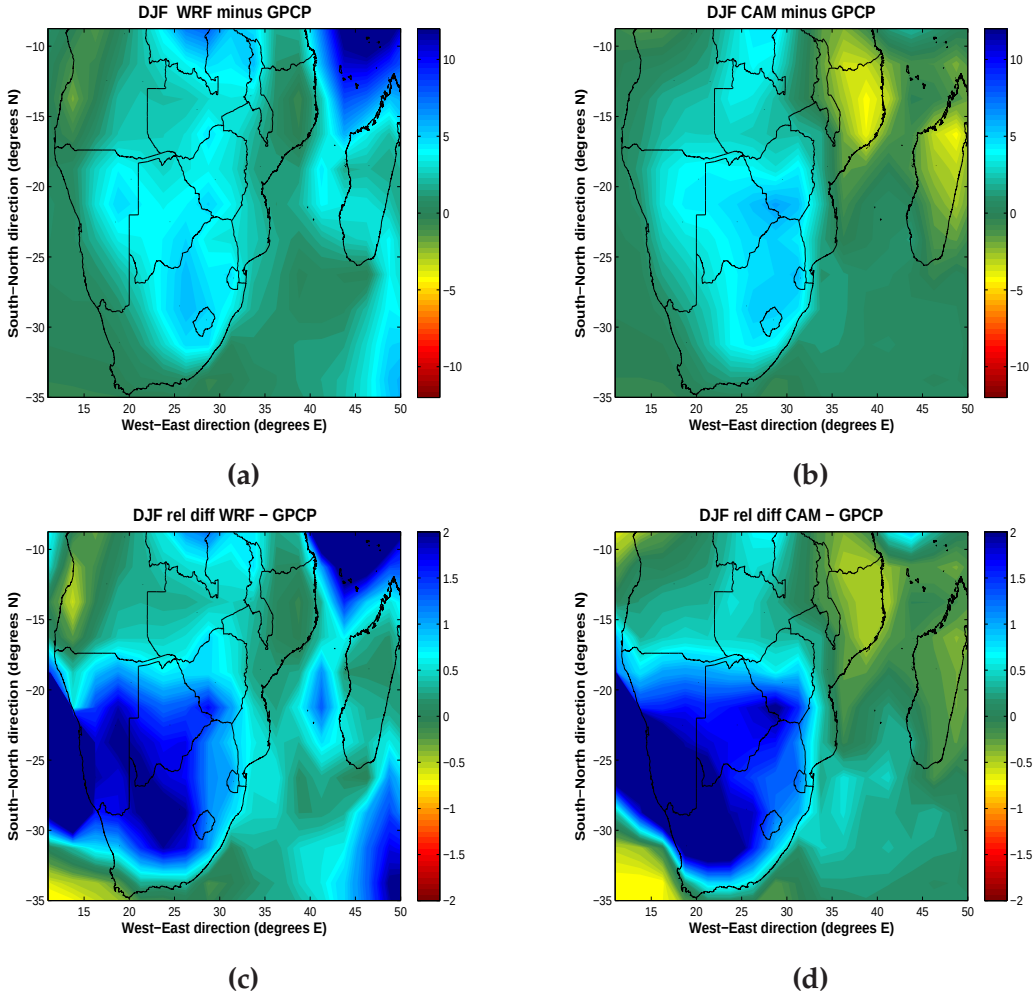


**Figure 4.7:** *Summer climatology (DJF) for differences in precipitation between WRF and CAM compared to observations. Figure a) difference WRF - GPCP (mm/day) b) difference CAM-GPCP (mm/day) c)WRF relative difference (WRF - GPCP) / GPCP and d) CAM relative difference(CAM - GPCP) / GPCP*

The rainy season falls within the months of DJF for the greater parts of southern Africa. The mean seasonal deviations in WRF and CAM with respect to GPCP are plotted in (Fig. 4.7), for DJF over 1991-2008. The general impression from Figure 4.6) is that WRF is overestimating the rainfall rate in the summer season (by up to 5.5 mm/day bias on the southern plateau and 11.0 mm/day in the Mozambique Channel)[10]. The overestimation in WRF is similar to CAM, although off somewhat less magnitude and covering a smaller area of the plateau in WRF. CAM is underestimating by about 4.2 mm/day in northeastern Mozambique, where WRF seems to represents the rainfall rate quite adequately compared

[10]Note that in the northeastern parts of the domain, is the area where the observational data contains the largest errors, up to 2 mm/day.

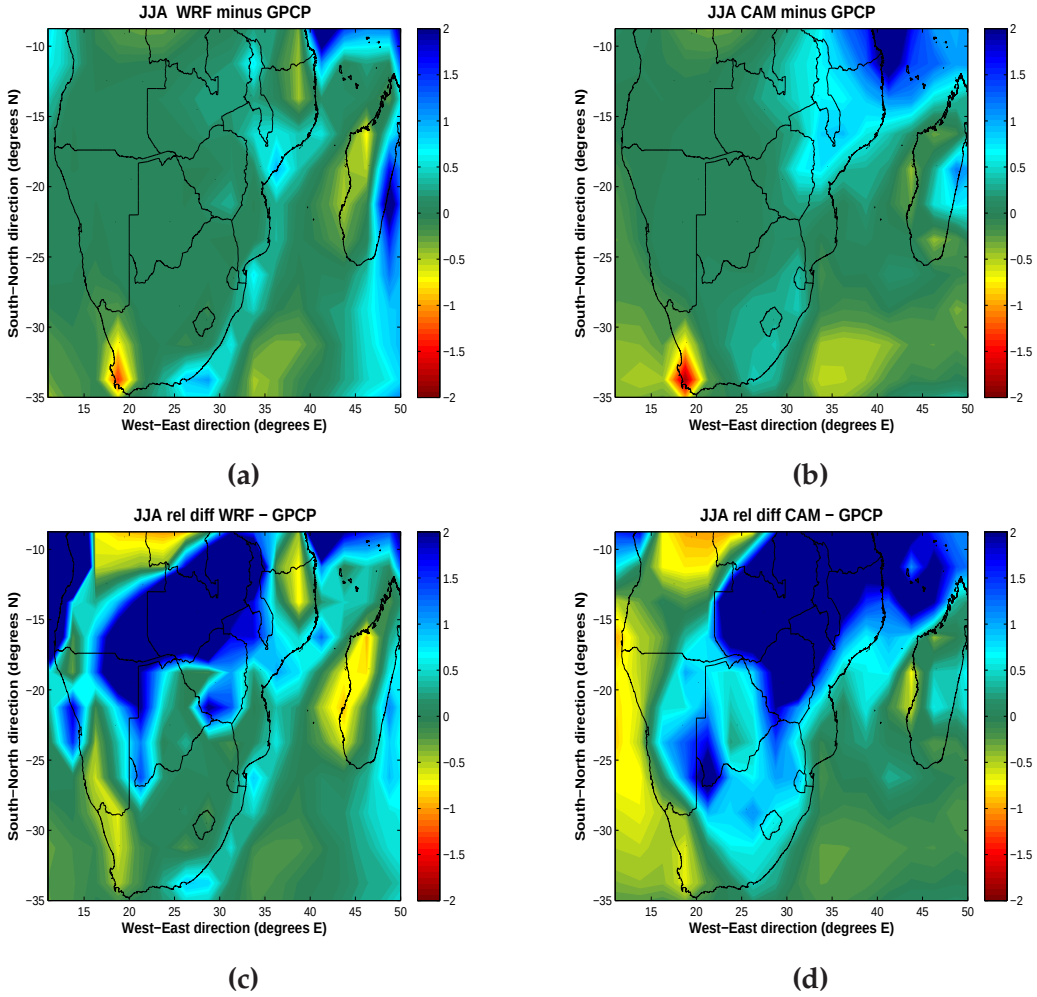


**Figure 4.8:** *Winter climatology (JJA) for differences between WRF and CAM compared to observations. Figure a) Difference : WRF - GPCP (mm/day) b) Absolute difference CAM -GPCP(mm/day) c)Relative difference (WRF - GPCP) / GPCP and d) (CAM - GPCP) / GPCP*

to GPCP. On the southwestern coast of Angola, WRF is underestimating slightly (maximum negative mean bias of to 1.9 mm/day).

As seen in the previous section, WRF appears to have a positive bias of latent heat over the southern African continent, implying a too strong Walker circulation. As there is access to lots of moisture in the rainy season, a stronger Walker cell over southern Africa will potentially lead to a stronger ascent over land and improve the precipitation efficiency, thus release even more accessible moisture. Hence this will provide a positive feedback mechanism that can cause an overestimation of precipitation over time, such as is seen in WRF. The circulation bias could possibly be inherited from CAM (see Figure 4.2, further discussed in section 4.3). Generally, most of the precipitation in the summer season is produced by the major rainbands mentioned in Section 2.1.1. Reason (2006) found that a modula-

tion of the Angola low could significantly affect the precipitation in Angola, Namibia and through to southern Africa, as the rainbands stretching over the plateau are fed by the low-level moisture in this region. Thus it could be suggested that this area is especially sensitive to a biased convergence zone. Additionally, the slight dry bias in WRF along the coast of Angola could be caused by increased moisture convergence from the northwestern parts towards the strong Angolan low.

The precipitation over the northeastern parts of the domain in summer draws special attention, as this is where WRF and CAM deviates the most. Discussed in Section 4.1.1, the precipitation intensity along the northeastern coast and in the adjacent Indian Ocean are highly sensitive to SST and moisture anomalies[11]. Thus the spatial distribtion of rainfall over this area is difficult to model. Northern Mozambique has the highest observed rainfall rate in the entire domain (during summer), and WRF seems to be reproducing the amount of precipition quite successfully. The convective scheme (Kain-Fritsch) used in the WRF simulation, is known to perform well in cases of severe precipitation (see section 4.3 and UCAR-edu (2010)), and can possibly explain WRF's skill in this area. The differences in WRF and CAM over this region will be further dicussed in Section 4.2, under Region 3.

Overall for JJA, WRF represents the regional precipitation patterns of this seasonal cycle very well. Figure 4.8 shows that the bias in WRF is somewhat less than in CAM with respect to GPCP. Although underestimating to some degree in northeastern Mozambique and Angola, WRF shows improvements compared to CAM. Still, on the southwestern tip both models fail to fully capture the increase of precipitation induced by the westerlies stretching northwards in winter time (WRF and CAM have negative biases up to 1.3 mm/day and 1.8mm/day respectively). The underestimation continues along the southern coast of Namibia in WRF, where CAM is closer to GPCP. The strong Kalahari high pressure in WRF (seen in Section 4.1.1) could suppress the northward movement of the westerlies, and thus possibly explain why the winter precipitation in southwest is underestimated in WRF (westerlies are associated with cold fronts and cut-off lows, thus precipitation. See Section 2.1.1).

Along the southeastern coast, the rainfall rate is slightly overestimated in WRF. This could be caused strong land-sea temperature gradient following the southeastern coastline in WRF, seen previously (Figure 4.4b).

Generally, the relative differences are larger in the southwestern parts for DJF and northeastern parts for JJA, which is mostly a result of relative difference being more sensitive the less precipitation there is. Nevertheless, for a utilisation of WRF in a future run, a smaller deviation in

[11] It should be reminded that GPCP generally contains a random absolute error of 2mm/day in this area (around 20% of the recieved rainfall).

| | WRF | | | | CAM | | | |
|---|---|---|---|---|---|---|---|---|
| | JJA- N | JJA- S | DJF -N | DJF -S | JJA- N | JJA- S | DJF -N | DJF -S |
| MAB | 0.26 | 0.19 | 2.48 | 1.95 | 0.39 | 0.22 | 2.10 | 2.11 |
| RMB | 2.30 | 0.44 | 0.51 | 1.62 | 2.32 | 0.61 | 0.42 | 1.40 |
| RMSE | 0.50 | 0.32 | 3.07 | 2.57 | 0.69 | 0.33 | 2.45 | 2.78 |

**Table 4.1:** *Spacial (computed for each grid before averaged) mean absolute bias (MAB), relative mean bias (RMB) and root-mean-square-error (RMSE) of precipitation (mm/day) between WRF and CAM relative to GPCP, for the southern African continent divided in two: Northern parts (19 ° S and north wards) and southern parts (19 ° S and south wards) See Figure 4.9.*

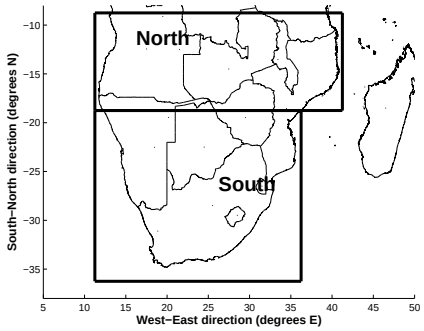


**Figure 4.9:** *North and south division of the continent for calculations of bias and RMSE.*

scarce precipitation could be just as important as larger changes in heavy precipitation. The agriculture is highly depended on the small amounts of precipitation, especially perennial crops (only a question of enough available moisture for survival in the dry seasons). When focusing on selected regions of southern Africa for future runs, the relative difference between the two runs is highly valuable climate change indication.

The spatial[12] mean absolute bias, relative bias and RMSE of precipitation are summarized in Table 4.1, where the continent is divided into a northern and a southern part (see Figure 4.9). Generally Table 4.1 recapitulates what is seen in Figure 4.8 and Figure 4.7; The seasonal representation of precipitation in WRF is slightly better than in CAM, except in the northern region in DJF where WRF has a larger bias than CAM.

## 4.2 Regions: seasonal cycle and interannual precipitation

In this section the domain is divided into 9 areas of interest (see figure 4.10 ), and the outputs are area-averaged over each region. The choice of regions are based on a combination of several factors: Topography (Figure

[12]Spatial is defined as computations performed on GPCP grid point level

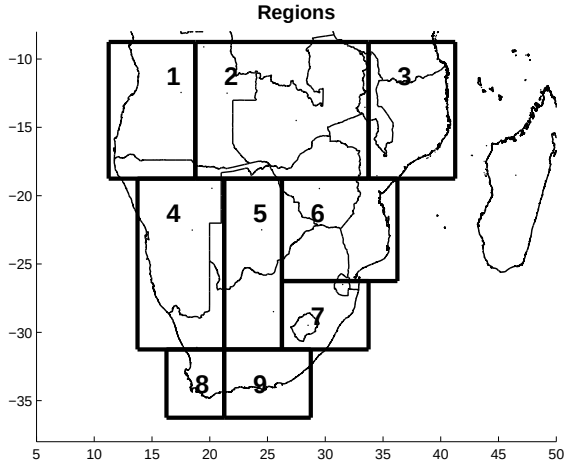


**Figure 4.10:** *Overview of the regions which the continent has been divided into.*

4.1), climatology (Figure 2.2) and previous studies (e.g Engelbrecht et al. (2008)). The same method used in section 4.1.2 is utilised here to average the WRF and CAM results over the larger grids in GPCP (2.5°x 2.5°), before selecting regions. In the following, the discussions can be assumed to regard precipitation, if other is not stated.

Monthly means and standard deviation of precipitation for 1991-2008 are computed for each region. Assuming normalised distribution, standard deviation is computed by

$$s = \sqrt{\frac{1}{n-1}\sum_{i=1}^{n}(x_i - \bar{x})^2} \tag{4.2}$$

, where n his number of years (=18), $x_i$ the monthly mean of year i, and $\bar{x}$ is the average of the monthly means over the 18 years.

Region 1-3 are the northern parts of southern Africa, region 4-7 the central southern Africa, and region 8-9 the southern tip (southern South Africa). The general impression from Figure 4.11 and Figure 4.12 is that WRF successfully captures the seasonal precipitation cycle in southern Africa. However, WRF overestimates from October to April in all the regions, except for the south-western tip (region 8). In total, WRF is somewhat closer to observed values than CAM, although for specific months and regions the opposite does occur. The general seasonal cycle for each region are briefly outlined in the following, and selected areas holding specially interesting results are discussed.

Both Region 1 and Region 2 are summer rainfall regions. Situated in the

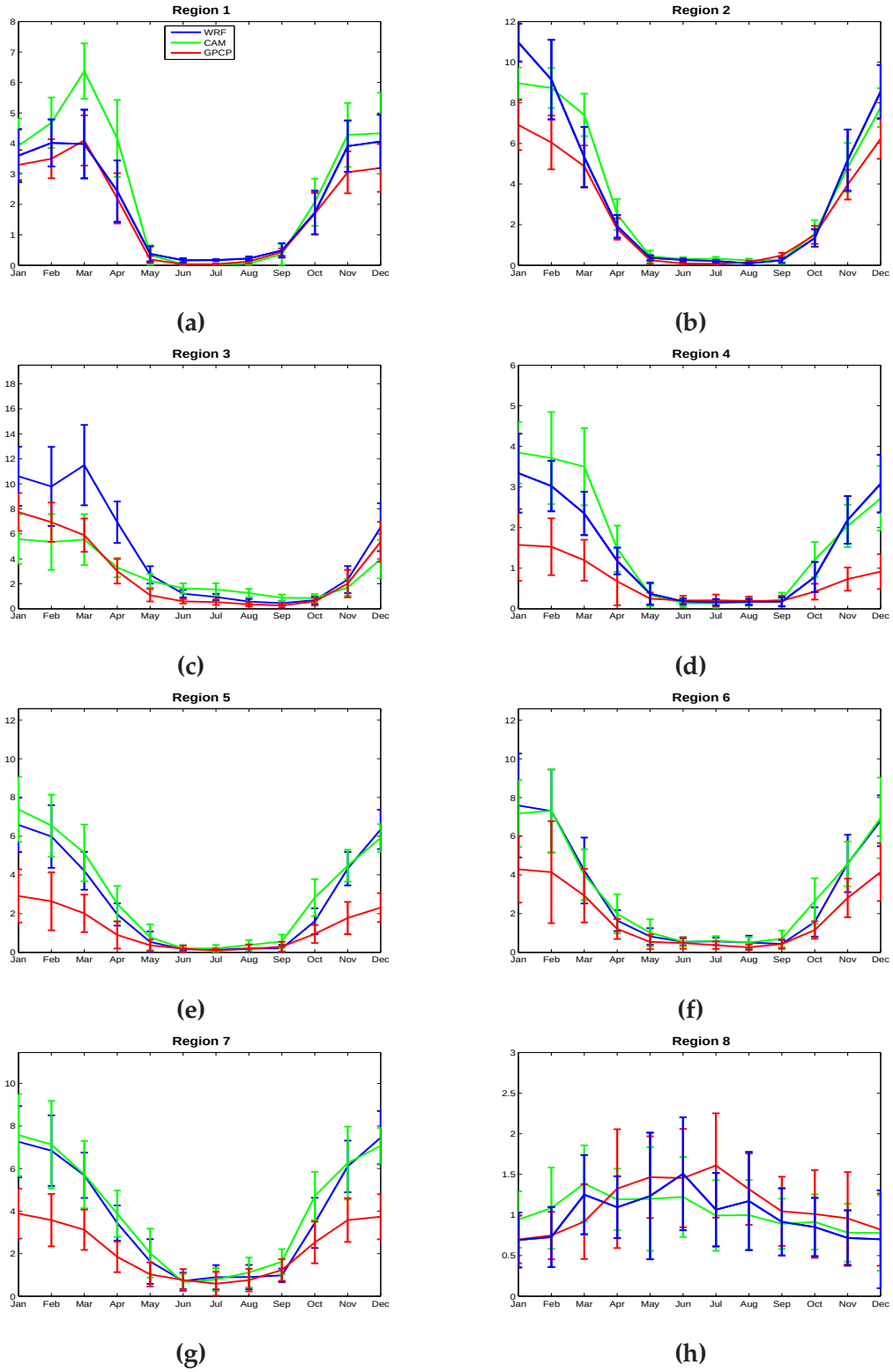


**Figure 4.11:** *Long term monthly precipitation means (mm/day) over 1991-2008 for WRF (blue), CAM (green) and GPCP (red). Notice that the range of the axes vary.*

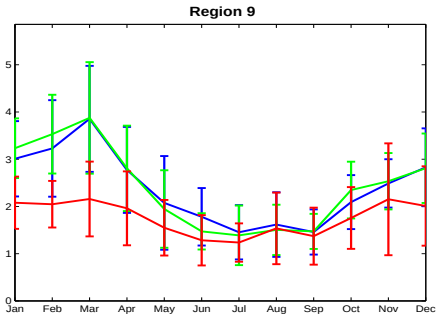


**(i)**

**Figure 4.11:** *(continued).*

"tropical wet and dry", these regions have close to zero precipitation during the winter season. A rapid increase of precipitation from September can be seen in Figure 4.11a, as the ITCZ moves southwards with moist air and ascending conditions in September. Region 1 and 2 reaches their maximum values respectively in March (4.1 mm/day ) and January (6.9 mm/day).

WRF simulations for Region 1 provides the best results of all regions. WRF successfully reproduces the seasonal variations in Region 1, reaching the same maximum of 4.1 mm/day as observed values, although reaching it in February. While overestimating from September to May, CAM is actually reproducing the exact observed values at a minimum of 0.03 mm/day in June and July, where WRF is overestimating (0.2 mm/day in June and July).

In Region 2, WRF manages to simulate low enough precipitation in winter time. Observed values have a minimum at 0.07 mm/day in July, while WRF reaches 0.08 mm/day in August. WRF correctly finds the maximun in February but overestimates with 4 mm/day (59% more than observerd). CAM is overestimating less than WRF at the maximum (3mm/day), however holding a large wet bias than WRF from February to October. One could question if a possible overestimation of the Lake Malawi temperatures could induce the wet bias in WRF over this region.

Region 3 is the summer rainfall region with the highest maximum precipitation (7.7 mm/day in January), receiving additional moisture from the Indian Ocean in summertime. As in section 4.1.2, Region 3 (Figure 4.11c) stands out as an area where WRF and CAM deviate the most (clearly seen in Figure 4.12c). WRF is overestimating and CAM is underestimating [13]. From June to October, WRF is closer to observed values than CAM. Both models are simulating the rainfall cycle in region 3 satisfactorily, although

[13]Comparing with figure Figure 4.7 and Figure 4.8 one have to keep in mind that the plots over monthly means are averages over larger regions. Even though the areas of wet bias in Region 3 are small, the values are large, thus the mean over Region 3 results in an a total overprediction in WRF.

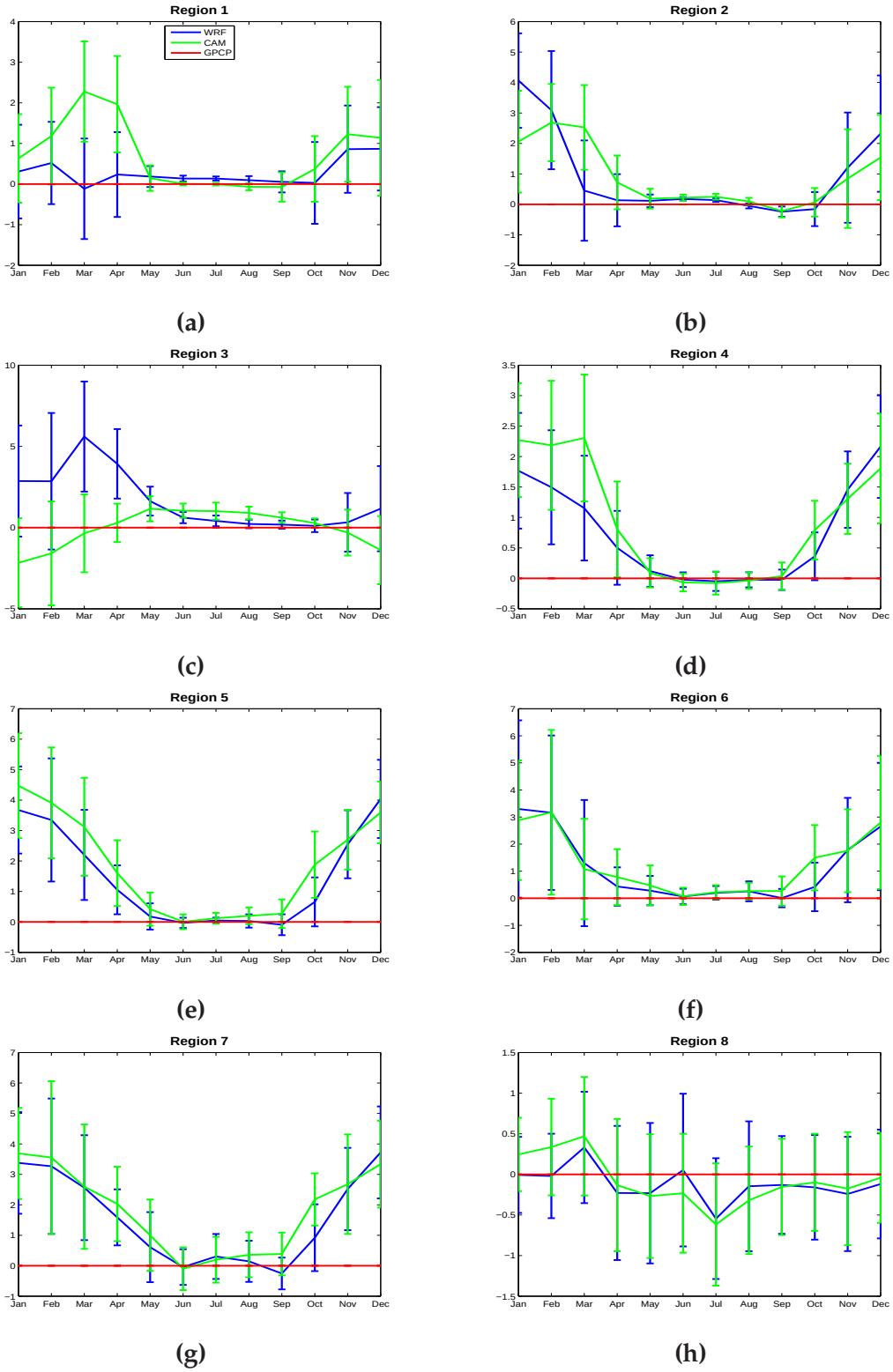


**Figure 4.12:** *Difference for the monthly means (mm/day) over 1991-2008 between WRF -GPCP (blue), CAM -GPCP (green) and GPCP-GPCP (red).*

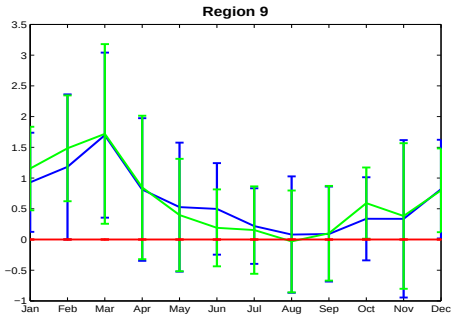


**(i)**

**Figure 4.12:** *(continued).*

the less sharp decline of precipitation from February to March in the observed data, is simulated as a rise in rainfall both in CAM and WRF. WRF has such a sharp increase that the annual maximum is reached in March at 11.50 mm/day (95% higher intensity compared to observed values in March).[14]

Tropical cyclones (presented shortly in Chapter 2), play an important role in the summer season climate in Region 3. They are associated with extreme precipitation. A possible cause for the overestimation in the Indian Ocean and Mozambique Channel during the summer seasons, could be due to an over-respresentation of cyclones, either by reproducing too intense or too many cyclones. Precipitation intense cyclones might also explain the larger standard deviations seen in WRF in Region 3 from December until April. This can be followed up by looking closer into daily outputs [15], or running with a storm-tracking option available in WRF (Wang et al., 2007). The tropical cyclones could also explain the differences seen in WRF and CAM, as the grid resolution in CAM might be to coarse to capture such extreme events[16].

Region 4 is also a summer rainfall region, but as most of the moist air from the Indian Ocean rains out traveling over the Blackenberg mountain range in the east, Region 4 is relatively dry and parts are defined as desert (see Figure 2.2). CAM and WRF are successfully reproducing the seasonal precipitation cycle, with the onset of the rainfall season in September and the rapid decline from March to May. Both models are overestimating, but WRF is closer to observed values (except in December).

[14]Note, as mentioned in Section 4.1, that it is wihtin the summer season in this region that GPCP has the highest absolute error (2mm/day).

[15]The wind tracks of the cyclones will be averaged away in long term seasonal averaging, while the extreme precipitation could still leave traces, possibly seen here.

[16]Coarse resolved GCMs are known not to capture tropical cyclones, or if they do, produce unrealistically low precipitation.

Region 5 is situated in the middle of Botswana and South Africa, with subtropical humid and desert climate (Figure 2.2). The seasonal precipitation cycle has the same pattern as Region 4, only holding more precipitation. Both CAM and WRF are correctly reaching the maximum and minimum precipitation in January and July, but are overestimating as much as 4.5 mm/day and 3.7 mm/day respectively in January, thus WRF is closer to observed values.

Region 6 is situated on the eastern coast and receives moist, warm air from the spring and onwards. Hence rainfall rate rises sharply in September to reach its maximum value in January (4.3 mm/day). Although overestimating, WRF correctly indicates the month of the maximum rainfall rate (7.6 mm/day in January). Region 6 has dry winters, with a minimum in August (0.3 mm/day). WRF reaches its minimum a month to late (0.4mm/day in September).

Region 7 also has summer seasonal rainfall, starting in September and ending in May. This region holds the highest point in southern Africa (Mount Njesuthi in the Drakensberg mountain range, at 3446m m.s.l), thus precipitation follows when humid warm air flow in from the southern Indian Oceans in the summer season, although with less intensity than in Region 6. Situated further away from the southern summer ITCZ, in additional to the surface winds that swipes over the Indian Ocean are bent northwards around Madagascar, less precipitation is produced in Region 7 compared to Region 6 (Engelbrecht et al., 2008; Taljaard, 1998). CAM and WRF follows the seasonal cycle fairly well, reproducing the sharp increase from September, stabilizing from December to March, and sharply declining again. Both models are overestimating from September to May and the maximums bias in WRF is 3.6 mm/day (in December).

Region 7 har been isolated to explore WRF's ability to simulate precipitation in high elevated regions. Previous studies have indicated that WRF overestimates in mountain areas(see Section 1.2), thus the overestimation are somewhat excepted. A testrun (not shown) using a hydrostatic option in WRF, induced an enhanced positive bias in this region, suggesting that a non-hydrostatic model does reproduce the rainfall rate in this area more successfully.

The positive biases from October to May seen throughout Region 4-7, are all possibly linked to the overestimation of convergence and thus a stronger moisture feeding for the major cloud bands stretching over theres areas (discussed in Section 4.1, see Figure 2.4).

Region 8 is a winter rainfall region where the rainy season starts in April and ends in September (Engelbrecht et al., 2008; Taljaard, 1998). Both CAM

and WRF simulate an early onset of the rainy season (March). CAM fails to produce a further rise in precipitation, while WRF follows the observed precipitation more closely, again peaking too early in June instead of July. As seen in Figure 4.12h, the biases in the models are small compared to the other regions. The underestimation on the southwestern tip was discussed in the previous section, probably being a result of westerlies situated too far south.

Lastly, the south-eastern tip (Region 9) is more of an all season rainfall area. The observed plot shows three maximums (March, August, November) and two minimums of monthly means (July and September). CAM and WRF simulations follows this annual rainfall cycle fairly well, although overestimating especially during late summer and fall. WRF and CAM have relatively similar outputs.

Figure 4.12 shows the absolute differences between the models outputs and observational data. It emphasizes what is seen in Figure 4.11 and the discussed results above.

**Interannual variability**

The standard deviations in Figure 4.11 represent the interannual variability of each month over the 18 years of focus. In northern and central regions, the observed standard deviation are larger in magnitude from September to March. Many factors are contributing to a great interannual variability of southern Africa (see Section 4.1.1), however in winter the prevailing high pressure over the continent creates stable dry and cool conditions, thus holding generally lower variability. In southern South Africa (Region 8 and 9), the standard deviation differs less over the twelve months, a region primarily influenced by the westerlies, cut off lows and SST anomalies.

Mason and Jury (1997) claim that SST anomalies in the Indian and South Atlantic Oceans can affect the tropical and temperate atmosphere circulation and moisture fluxes over the southern Africa and significantly influences the rainfall variability[17]. As both CAM and WRF are forced by observed SSTs, it is intriguing to investigate the representation of the interannual variability in the models compared to GPCP.

CAM and WRF do not show any critical deviations from GPCP concerning the standard deviation (see Figure 4.11). The mean standard deviation

[17] A wealth of work have been performed concerning the SSTs influence on rainfall variability, but will not be outlined further than in Section 4.1.1

over all regions for GPCP, CAM and WRF are respectively 1.2 mm/day, 1.5 mm/day and 1.7 mm/day (generally Region 3 is increasing this for WRF). This infers that the interannual variability of precipitation are to some degree within the same magnitude as observed, but does not provide information of the temporal correlation. Thus, the correlation between 1998-2009 seasonal mean for CAM/WRF and observed (GPCP) are computed over each region (see Table 4.2) for summer (DJF) and winter (JJA). The correlations in Table 4.2 will only be discussed briefly here.

Previous studies running RCMs forced by reanalysis data show varying interannual correlations (0.3-0.7), overall quite low or even non existent in some areas (negative) (Giorgi et al., 2011; Engelbrecht et al., 2008; Sylla et al., 2010). Reanalysis data are of better quality than CAM, thus low correlations were anticipated from this study. As expected, the correlations (winter to winter and summer to summer variations) in WRF are overall poor. In DJF they are generally below 0.3 and in some regions negative, but for JJA the correlations are somewhat better (ranging between 0.2-0.5, except Region 1). For JJA, CAM and WRF show relatively similar results, but in DJF CAM represents the interannual variations better than WRF. Especially in Region 4 and 5, the correlations are relatively high in CAM. Plots of the interannual variation of the winter and summer seasons over 1991-2008 can be found in Appendix B, Figure B.1 and B.2.

As seen from Section 4.1.1, several interacting processes form the interannual variability in southern Africa. The correlations in Table 4.2 suggests that the models fail to skillfully reproduce this variability over Region 1-3 and 7-9, implying that SSTs are not the governing forcing factor of interannual variability. However, the relatively high correlations seen in CAM for Region 4 and 5 suggests that over these regions, SSTs are influencing interannual variability to a larger extent.

A full comparative study of the correlations requires a more comprehensive analysis of the model physics and the underlying processes of interannual visibilities in southern Africa.

## 4.3 Testruns with different scheme options in WRF

When it became clear that the future runs would not be analysed thoroughly (explained further in Sec 4.5), it opened up time and saving space to test other scheme choices in shorter runs. Two additional sensitivity tests have therefor been performed, by changing one of the physical scheme options (the scheme options are described in section 3.3.3). In the first testrun a different cumulus scheme option was employed (Grell vs Kain) and in the second, the planetary boundary layer scheme was changed (MYJ vs

| MODEL Region | WRF COR DJF | WRF COR JJA | CAM COR DJF | CAM COR JJA |
|---|---|---|---|---|
| 1 | -0.03 | -0.09 | -0.19 | -0.23 |
| 2 | 0.04 | 0.29 | 0.31 | 0.11 |
| 3 | -0.63 | 0.21 | -0.32 | 0.26 |
| 4 | 0.28 | 0.36 | 0.59 | 0.14 |
| 5 | 0.21 | 0.45 | 0.46 | 0.34 |
| 6 | -0.14 | 0.21 | 0.11 | 0.27 |
| 7 | -0.03 | 0.30 | 0.26 | 0.43 |
| 8 | -0.17 | 0.25 | -0.20 | 0.20 |
| 9 | 0.12 | 0.21 | 0.29 | 0.15 |

**Table 4.2:** *Area-averaged correlation coefficients of interannual variability between observed (GPCP) and modelled (WRF and CAM) over the summer(DJF) and winter(JJA) months.*

YSU)[18]. All other options remains as in the historical run.

The testruns was primarily computed to retrieve more information of possible weakness for the originally chosen scheme options, although they are important for guidelines in possibly additional longer runs(see section 4.5). The results in previous sections points out that WRF has the largest biases with respect to observations within the summer season (although underestimating in wintertime in South Africa), and generally the largest deviations from CAM is also seen in DJF. Hence, a summer season is chosen to be analysed here (DJF 1990/1991).

The simulations are computed from 1. January 1990 to 28. February 1991, and only summer season means for DJF are plotted here ( December 1990, January 1991 and February 1991). In Figure 4.13 the historical (thoroughly described in the methodology chapter) is now only plotted for DJF 1990/1991 and denoted as the control run. The different test runs are named after the schemes changes (Grell and MYJ).

In Figure 4.13 the results from respectively the control, Grell and MYJ are plotted for DJF 1990/1991. Grell generally simulates precipitation on the plateau very well with respect to GPCP. Although not to the same extent as the control run, Grell also overestimates in the northern Mozambique Channel. In section 4.1.2 the bias over the plateau was suggested to be connected with the strong low-level convergence. Looking at the pressure heights in Grell (not shown), the low level convergence is less strong

[18]Changing land surface scheme (LSM) would also be an interesting study, but requires a change in the soil layer input data, and was therefor not prioritised. Additionally, Crètat et alt 2011 also showed convective and PBL scheme changes made the largest contribute to precipitation differences

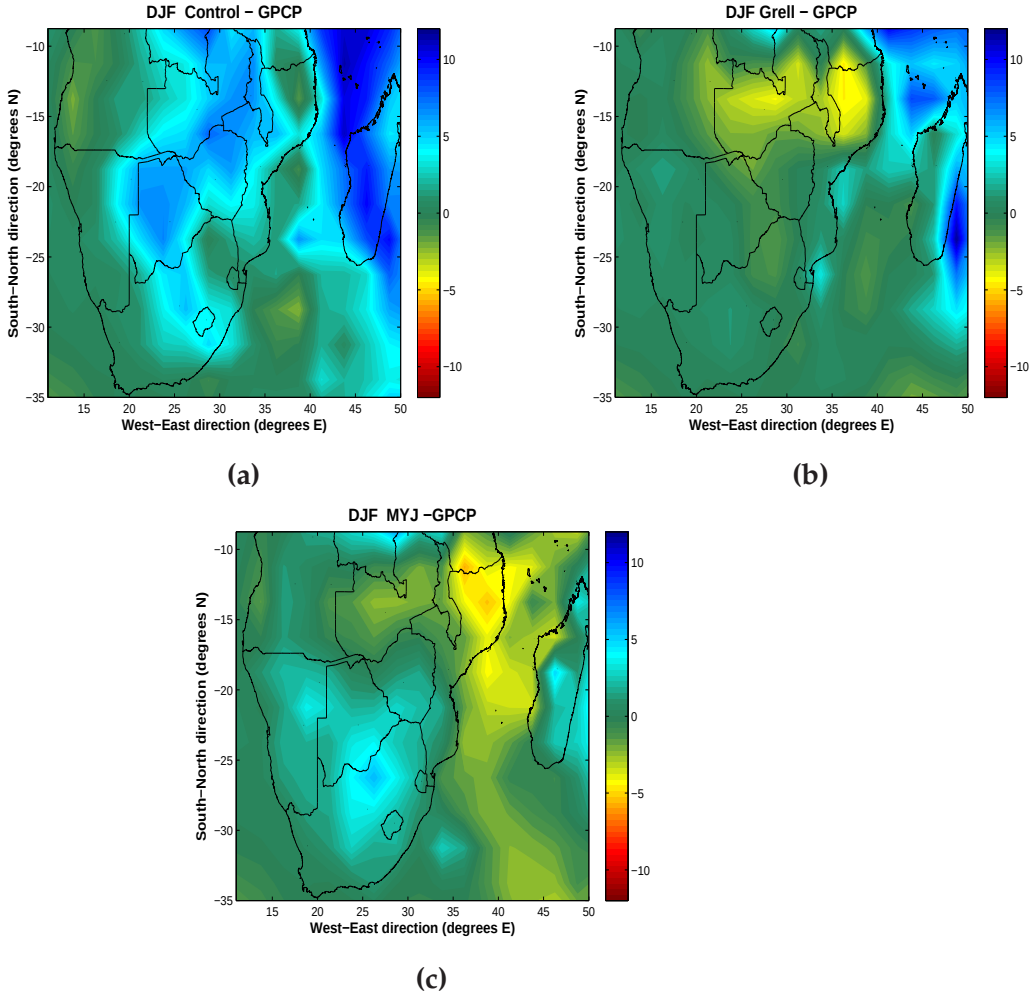


**Figure 4.13:** *Absolute difference in precipitation (mm/day) between the various WRF scheme options and GPCP for DJF 1990/1991 means (December 1990, January 1991 and February 1991). WRF outputs are averaged over GPCP grid boxes. a) original, b) Grell and c) MYJ*

compared the control run, hence possibly a reason for the more successfully representation of rainfall rates over the plateau. Under certain circumstances Kain-Fritsch scheme (convective scheme option in control run) is known to leave unrealistically deep saturated layers(UCAR-edu, 2010), which can possibly cause stronger ascent, hence low-level convergence and more intense rainfall. This leads to a stronger Walker circulation and thus a positive precipitation feedback mechanism. Additionally, extensive moisture will feed the rainbands stretching over the southern African plateau.

MYJ produce the same patterns as the control run over southern African plateau, although it is slightly less overestimating. The low-level convergence is stronger in MYJ than GPCP (seen from plotted pressure heights, not shown), though somewhat less than in the control run. In the Indian Ocean MYJ is underestimating, deviating substantially from the other two

runs.

Both Grell and MYJ are underestimating in northern Mozambique and westward towards Angola. Kain-Fritsch is known to produce good results in areas of heavy precipitation (see Section 4.1) and is possibly a better choice than Grell for precipitation over northern Mozambique. It is somewhat unclear why MYJ is underestimating in this region. Although, as MYJ also has a negative bias in the Indian ocean, it can seem like there is in general less moisture available in MYJ. 2m water vapor (not shown) does not provide any further information[19], but 10m wind (not shown) seems to have slightly less magnitude when curving around Madagascar towards Mozambique in MYJ. This could imply that less moisture is transported over the Indian Ocean and towards land in MYJ (at higher levels or at daytime as it is not seen in 2m water vapor) but further investigation is outside of the scope of this thesis.

The amplified low level convergence seen especially in the control run and thus the historical run, has been suggested to arise from errors in the forcing model CAM, as the geopotentials heights are similar in CAM and WRF (Figure 4.2). As the Angolan low is not amplified in Grell (and less i MYJ), this would contradict the assumption. Nevertheless, Sylla et al. (2011) suggested in a very similar study, that the strength of the low level convergence is driven by the lateral boundary conditions, and that the overestimations can be counterbalanced by adjusting different parameters in physical schemes.

| | Control | Grell | MYJ |
|---|---|---|---|
| Mean bias | 2.3 | 0.26 | -0.17 |
| Mean absolute bias (MAB) | 2.9 | 1.8 | 1.6 |

**Table 4.3:** *Bias in scheme options with respect to GPCP in mm/day, over the entire domain.*

In table 4.3 each of the WRF runs have been averaged over DJF, subtracted by observed values and then averaged again over the entire domain, both for mean bias and absolute mean bias. The MAB in the two testruns are somewhat less, thus both Grell and MYJ looks like interesting alternatives to the control run, depending on the area of focus.

One should be aware that responses to the model for specific setup options may not be apparent in short simulations and could become evident only over longer running periods, in addition to be different for selected seasons (Bukovsky and Karoly, 2009). As seen in Figure 4.13 a) and Figure 4.7, the bias from GPCP in DJF 1990/1991 and DJF 1991-2008, has the same patterns of overestimation. Thus for this setup, the short term analysis looks quite representative for the DJF 1991-2008, and possible the same is true for

[19] Note that these values are for 00:00 UTC

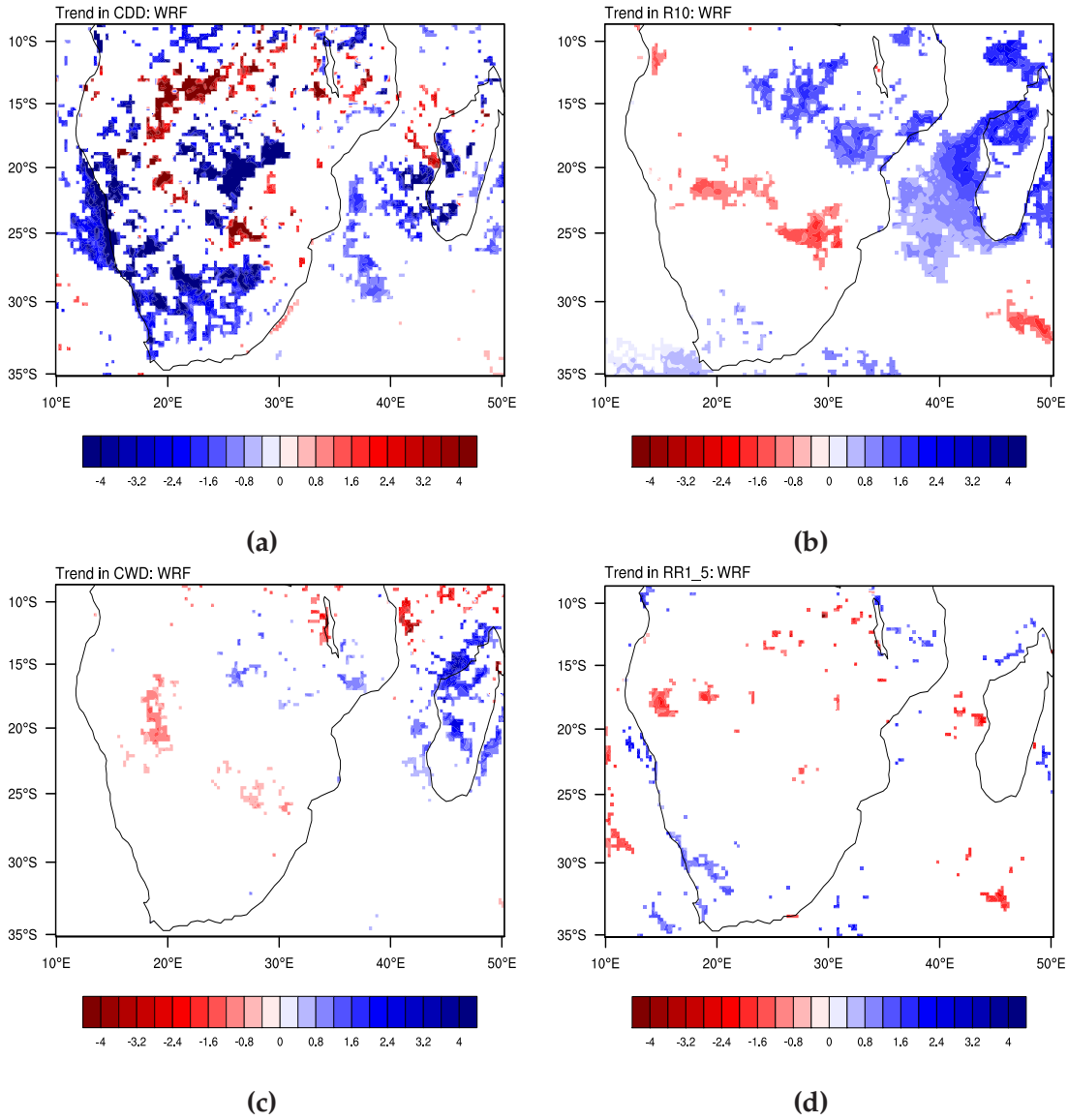


**Figure 4.14:** *Trends (number of days/year) in WRF for 1998-2009, calculated on a 90% significants level for a) CDD, b) R10, c)CWD and d)RR1_5. The trends plott for TRMM data can be found in Appenix C, Figure C.1.*

Grell and MYJ, although this is not a necessary a direct consequence.

## 4.4 Changes of extreme precipitation

A change in extreme weather poses a great challenge for agriculture in a future changing climate. SST anomalies are thought to be one of the main driving forces behind extreme events (e.g ENSO and cyclones), thus they are to some extent expected to be evident in regional climate modelling

forced by observed SSTs. Nevertheless, research on changes in extremes are specifically limited over Africa in either models or observations, as investigations of extreme events requires high resolution daily data for a long time period(IPCC, 2007). One of the advantages of the high resolution dataset retrieved from a WRF run is precisely its feasibility for use of extreme trend analysis.

Comparing extreme precipitation in a future and a historical RCM run, can provide a future projection of changes in extreme weather events. Additionally it is interesting to look at extreme trends within a future run. Thus a validation of the changes in the extreme events within a historical run with observed SST forcing is valuable. If the aim here was to retrieve the best knowledge of extreme trends in the historical run, observational or reanalysis data would rather be analysed. Thus it is important to state that this section is not intended to provide high quality trend indices over the years of focus, but to show WRF's applicability for climate trend analysis.

Precipitation based climate indices in WRF are calculated for 1998-2009, in order to draw a comparison with an ongoing study (Sukumaran, 2011) using Tropical Rainfall Measuring Mission precipitation data (TRMM)[20] TRMM plots provided by Sandeep Sukuruman, can be found in the appendix, see Figure C.1. In this section the terms trends and changes are used interchangeably, although trend is usually employed for longer time periods where it is possibly caused by an external forcing (e.g anthropogenic)[21].

The indices shown in Figure 4.14 are:

| Index | Description |
|---|---|
| RR1_5 | Number of days with precipitation between 1 and 5 mm |
| R10 | Number of days with precipitation 10 mm and above |
| CWD | Maximum number of consecutive wet days |
| CDD | Maximum number of consecutive dry days |

General description of the different methods used to compute the trends can be found at `http://cccma.seos.uvic.ca/ETCCDI/list_27_indices.shtm`. The trends are calculated on a 90 % significance level using Generalized Linear Model (GLM) assuming a poisson distribution[22]. The statistical analysis and plotting (seen in Figure 4.14) are performed by Sandeep Sukumaran working on the SoCoCa project. Blue shade in R10 means that the

[20]TRMM measures rainfall using a combination of passive microwave and active radar sensors, and is provided by NASA. TRMM is a homogeneous precipitation dataset covering the entire tropics (its homogeneity has been questioned and is at the time being under research), with high resolution ( 0.25 °x0.25 °) gridded data covering a region of 40 ° N to 40 °.

[21]Trends within a 12 year run can not with certainty be caused by external forcings

[22]Detailed description can be found in (Gunwald and Jones, 2000; Little et al., 2009)

area is getting wetter while the red shade indicates drying. In CDD the colorbar is reversed, blue still stands for wetter trends and red for dryer (unity is nuber of days per year). Because a decrease in CDD[23] means the area is getting wetter (less days of less than 1mm, means more days of more than 1mm) and an increase in CDD results in a dryer trend.

Seen in Figure 4.14a, WRF mostly simulates a decreasing (wet) change of CDD in the southwestern parts of the domain (South Africa, Namibia, northern Botswana and southern Zambia). The wet trend is similar in TRMM, although on the western coast of Namibia, TRMM based indices are positive. Areas implying an increasing (dry) change in WRF are more scattered over the continent (Malawi and south African plateau). The indices of CDD in the Mozambique Channel are mostly wet in WRF, while being dry in TRMM (as seen from seasonal results in Section 4.1.2, this is in general an area where WRF contains biased precipitation means compared to observations).

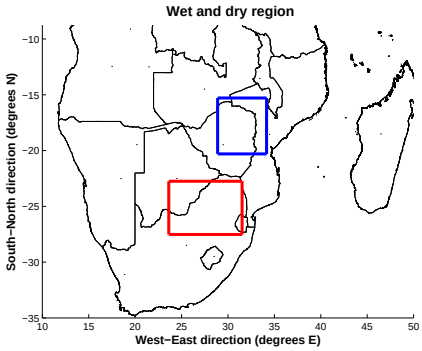


**Figure 4.15:** *Two areas are chosen for plotting a time series, wet (blue) and dry (red).*

The R10 trend based on WRF is found to be increasing in the southern parts and in the northeastern tropics north of 20 ° S (coinciding with trends in TRMM) and weaker negative trends can be seen over Zimbabwe and Botswana. Also evident here, are large deviations in the Mozambique Channel as WRF strongly indicates a wet trend, while the trend is mostly negative in TRMM. Additionally, there is a negative trend along the northwestern coast in TRMM that is not evident in WRF.

In Figure 4.14c and Figure 4.14d the indices of CWD and RR1_5 are weak, which corresponds with TRMM based trends, although RR1_5 indices in TRMM are stronger and expanding over a larger area in the southwest. It could also be noted that the weak response of CWD in WRF is generally of opposite sign in TRMM.

[23]Dry day is defined as the number of days with precipitation less than 1 mm

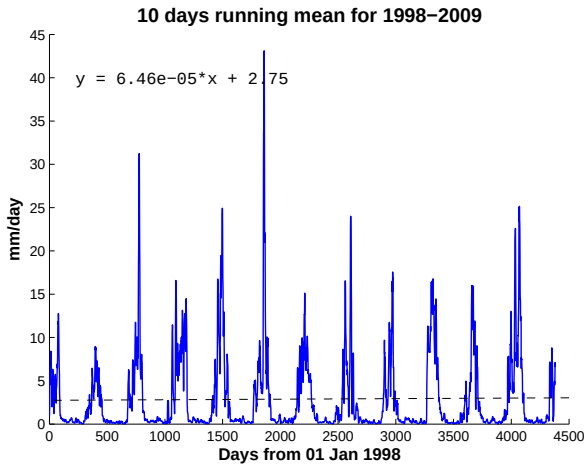


**(a)**

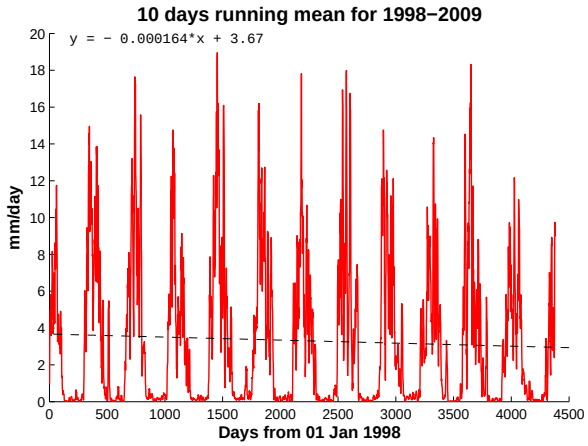


**(b)**

**Figure 4.16:** *Time series of 10 days running mean of the daily precipitation (mm/day) in WRF for 1998-2009 is plotted. The dashed line shows linear trend in mean precipitation. (a) is the wet area and (b) is the dry area .*

Two areas, called "wet" and "dry", in R10 has been chosen for further analysis, see Figure 4.15. The blue area (wet) and the red area (dry) respectively indicates an increasing and decrease trend in R10. Time series of an area averaged 10 day running mean of precipitation for 1998-2009 are shown in Figure 4.16, over the wet (a) and the dry (b) area. The wet area holds a slight increasing trend and the dry area a decreasing trend, thus comparing with R10 tendencies, the daily precipitation mean seems to change in the same direction as the extreme trends.

It is debated to which degree an extreme change analysis gives valuable results over a short (12 year) simulation, though Sukumaran (2011) claim that with high resolution, quality and homogeneity data, 12 years should

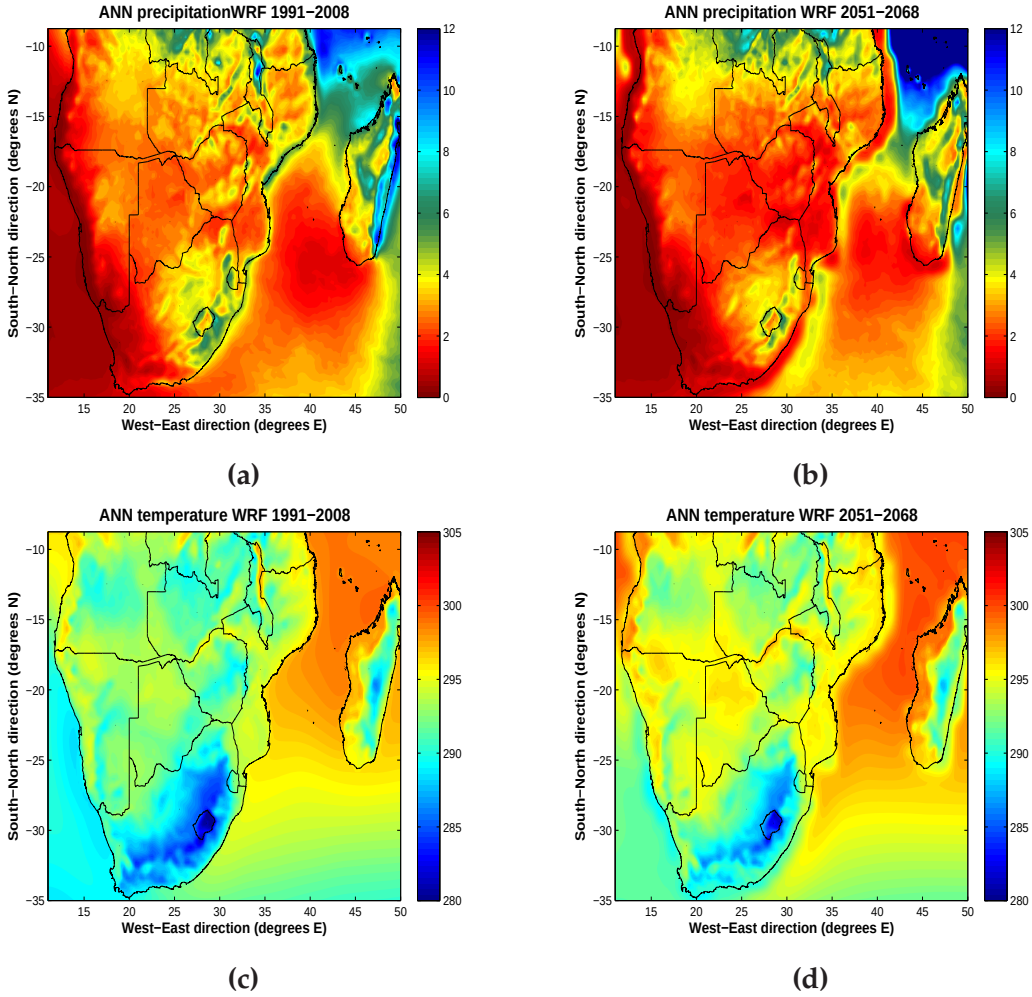


**Figure 4.17:** *a) Annual averaged precipitation (mm/day) (same method as Figure 4.7 and 4.8)) for a) WRF 1991-2008, b)WRF 2051-2068. Annual averaged temperature for c) WRF 1991-2008, c)WRF 2051-2068. The historical run is presented to clearly see the difference along the coastline.*

be sufficient for this application. Nevertheless, the linear change in Figure 4.16 are computed only to view how extreme events in longer runs can be linked to general mean changes. It requires longer time series to compute linear trends of high certainty (the 12 year linear trend could change signs from adding or subtracing one year). Although the statistical calculations are over a short time slice and only briefly analysed, the extreme changes in WRF seems to be reasonably well reproduced compared to TRMM.

## 4.5 Future runs

A full future run providing valuable analysis for the precipitation patterns in 2050-2069 could not be performed in this study, as it was discovered

errors in the input data from CAM. To solve this problem, CAM had to be rerun, which was beyond the time schedule for this thesis. Nevertheless, it was decided to finish the entire future run, to show the results and address the problem to give directives for later studies.Thus a few preliminary results from the testrun for the future (2050-2069) are presented here and guidelines for further work are made.

The results from the future time slice are presented in Figure 4.17 and Figure 4.18. A rim of unphysical low values of precipitation along the coastline in the ocean was spotted in the first results after a short running-period. The problem seems to arise from a slight difference in the landmask used in the SST forcing data[24] and in CAM's landmask. This resulted in a data gap of surface temperatures over some points in the ocean along the coastline, as land surface temperatures was displaced into grid cells in the ocean. Thus as CAM has an abrupt shift in temperatures in the oceans along the land/ocean boundary, this is adopted by WRF and also seen in the WRF simulations, Figure 4.17d.

As one can not be certain to which extent the low temperatures around the coastline is affecting the precipitation on the entire plateau, there is no reason to discuss or analyse the results from the future run. However, if the future simulation turns out to be similar after correction of the input data, they are overall corresponding somewhat to results from previous studies (see Figure 4.18), indicating dryer conditions in west and wetter in east. Regional details will be intersting to analyse and take into consideration when giving future climate suggestions, and should be performed thoroughly in a corrected future run.

## 4.6 Suggestions for further research

Dynamical downscaling of CAM by the use of WRF is still at an initial stage. Thus, as this is a first step to reproduce precipitation patterns in southern Africa forcing WRF with CAM, more research is in need in order to acquire satisfactory results. A few sources of the precipitation biases have been suggested in this chapter, although it requires thorough studies of other variables and additional sensitivity simulations to draw firm conclusions of the errors' orgins (biases might also arise from several interacting errors). Exploring the orgins of errors in this study is an initial step for furher work, and higher resolution observation data set would enhance the analysis. With this as a basis, improvements of input data from CAM, setup and parametrizations of WRF should be performed. Thus, suggestions for further research are presented in this section.

[24]The only change between the future and the historical runs are SSTs, greenhouse gases, aerosol and ozone input. As the SSTs was changed to modelled SSTs for the future runs (from HAdISST), the error arose only here, and not in the historical run

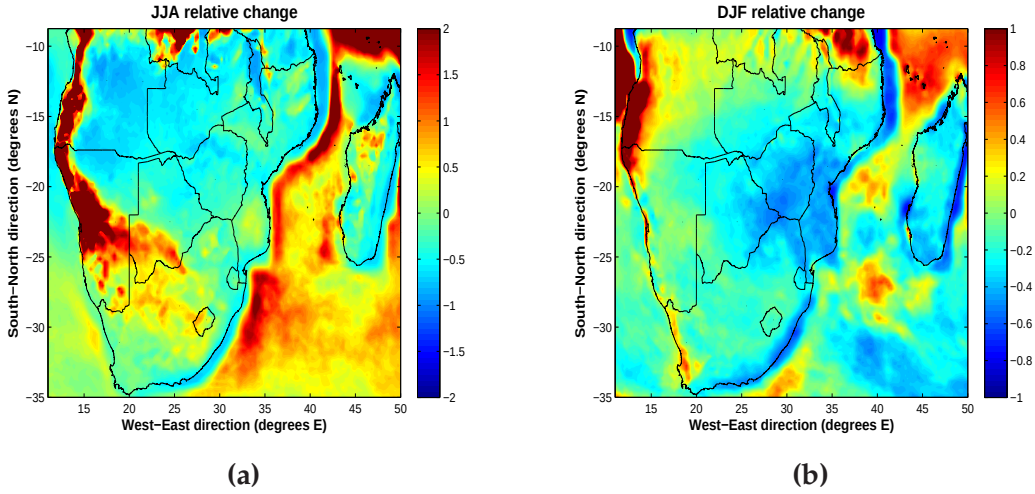


**(a)** **(b)**

**Figure 4.18:** *Relative difference between historical (1991-2008) and future (2051-2068) WRF run for a) JJA b) DJF ((future-historical)/historical)*

### Identify errors

In this study we have mainly focused on precipitation patterns. Further analysis and validation of variables (e.g water vapor, vertical wind, heat fluxes, cloud cover, long - and shortwave radiation) should be carried out at different levels, to get an in-depth impression of how WRF performs as a dynamical downscaler and also retrieve further information of the governing systems that lie behind the precipitation patterns. To carry out such a thorough analysis over a long simulation, there is a need for computational resources and storage capacity to output variables at least every 6 hours (as WRF outputs are instantaneous values, averages should contain values from different parts of the day). Additions to the source code were made in this study, to output a few variables averaged over each time step. More variables can be added to average while running, although this is a greater technical challenge than outputting several times a day. Performing shorter dedicated simulations of episodes, requires less computational resources and are highly valuable especially if run for periods where detailed observational data are available. Additionally, seasonal and interannual precipitation in this study should be analysed using higher resolution observational data (e.g TRMM data (1998-2009)), to obtain more information on a local scale. With such daily high resolution observational data, number of rainfall days versus intensity should also be investgated.[25]

Sensitivity studies using different scheme options in WRF (see scheme options in section 4.3) are important both to identify possibly weaknesses in the schemes, and to find the best possibly scheme combination for the domain of interest. As we wanted to compare a historical and a future

[25]The two latter suggestions would be the first "next step" to be performed in this thesis, but there was not enough time.

run driven by the same scheme options in WRF, the choices of scheme combination was not of main priority [26]. When the future run turned out to be unsuccessful, time allowed for two different scheme options to be tested, which strongly suggests that different physical parametrization might improve the simulations over some areas. Nevertheless, as southern Africa is a diverse and complex region, the testruns implies that different combinations of schemes might improve results in one region, while aggravate them in another. Additional sensitivity studies should be performed, preferably for a couple of years, to look at annual and seasonal outputs. It is suggested by previous studies that an ensemble mean over different combinations provides less bias compared to observations, and will carry through less noise in a future run.

Hudson and Jones (2002) suggest, as in this study, that the circulation biases are inherited from the GCM and point out that the key to improve the summer seasonal precipitation bias possibly lies in the GCM. In this study, it is obvious that different schemes have a large effect on precipitation, but as mentioned in Section 4.3, different parameters in physical schemes can counterbalance errors adopted from GCM, thus the results from the sensitivity runs do not necessarily imply that the errors only arise from small scale physics. To identify the origins of the precipitation overestimation in WRF, additional runs should be carried out, forcing WRF with global reanalysis data (e.g. NCEP[27] or ERA-Interim[28]) and compare with results from this study. This would provide valuable information to which extent the errors are adopted from the forcing at the boundaries or if they arise from small scale physics. Additionally, with better quality driving fields, one can to a larger extent explore how well WRF downscales, being less disturbed by adopted large scale errors.

**Improving simulations**

An ensemble of longer runs with WRF are extremely computationally heavy, and will possibly not be performed in the nearby future. Thus, one should strive to improve the scheme combination that represent southern Africa most successfully after sensitivity studies. The physics of each scheme should be analysed, to see if corrections can be made to enhance the simulations in southern Africa. For a comprehensive analysis, better observational data are also in order. In this study we have mostly used GPCP for verifying precipitation patterns in WRF. For a thorough model validation one should generally use different observational datasets (Sylla et al.,

[26] Assuming that a bias will be somewhat equal in both runs over the same areas, and thus not evident when subtracting the two runs from each other.

[27] National Center for Environmental Prediction

[28] ERA-Interim as initially described in ECMWF Newsletter No 110 is an 'interim' reanalysis of the period 1989-present in preparation for the next-generation extended reanalysis to replace ERA-40. ECMWF Newsletter Nos 111 and 115 contain further information (http://www.ecmwf.int/research/era/do/get/era-interim)

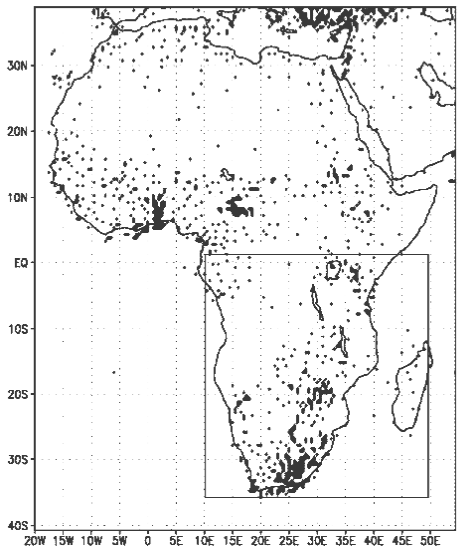


**Figure 4.19:** *GTS gauge dataset (note, from 1990-2000) over Africa.*

2010). Over particularly regions of interest, high resolution observational data should be employed, to obtain an in-depth verification. The coverage of gauge data are generally greatest in South Africa, while it is more limited over the larger areas of southern Africa (see Figure 4.19), (Layberry and Kniveton, 2000)). As reducing the uncertainties in the observational data will enhance the validation of the models and thus contribute to the work of improving them, obtaining better observations should generally be of a larger focus. Founding of observational campaigns would be of great value for regional climate projections in a complex area where agriculture is highly depended on the rainfall rate[29].

The location and size of the domain are important, seen both from this and previous studies (Landman et al., 2005; Tummon, 2011; Seth and Giorgi, 1998). Not including Madagascar in the initial test runs, resulted in extreme precipitation (up to 20mm/day in DJF seasonal mean) on the southeastern coast of Mozambique and east of Zimbabwe. It would be interesting to run with an enlarged domain, especially to see if the precipitation deviates from the historical run in the Mozambique Channel. Tropical cyclones ravaging in this area, are mesoscale phenomenon but significantly influenced by the large scale zonal flow. It is suggested by Landmann (2005) that this typical occurrence is represented very differently for various domain size and location.

This study focus on downscaling the global climate model CAM. WRF seems to generally produce somewhat better results than CAM concern-

[29]SAFARI-2000 has been the largest campaign to the date in southern Africa. Datasets from this campaign could be used to closer analyse the summer season of 2000 in this study.

ing precipitation. It could be considered to investigating if less/more frequent forcing at the boundaries would have a positive/negative affect on the result. Changing the nudging condition in the relaxation zone[30], by either specifying a higher decay factor (0.33 in this study) or changing the specified boundary condition to linear, could be a valuable further research.

Computing simulations of even higher resolution, generally for shorter time slices (due to computational restrains), should provide enhanced results. WRF also allows for horizontal nesting[31], which would be an interesting step further to focus on specific regions. As this is more computationally heavy, it was not computed in this study. However, nesting down to 9km x 9km (and further to 3km x 3km) for an inner domain is possible without considerable technical challenges. This would be a highly valuable tool for local regional climate research.

There is additionally ongoing work on coupling WRF with ocean models and develop more comprehensive treatments of land surface and hydrology processes, which would possibly improve WRF as a dynamical downscaler greatly(Qian et al., 2010).

**Future run**

Based on this and further studies, a full future run with WRF should be computed, investigated and compared thoroughly with a historical run, to look for future climate change signals. When analysing a future run, one have to keep in mind that biases and natural variability in one single run might disturb the climate signal. Although computationally heavy, this can be improved by running ensemble of simulations and using the ensemble mean for climate projections. Eventually, several runs with different greenhouse gas scenarios, variational land surface data (e.g albedo, vegetation) and alternative SSTs should be compared.

Finally, as mentioned in Section1.3, the simulations performed in this study have a secondary perpose of comparing with a similar ongoing research under the SoCoCa-project[32]. Thus, comparing these two studies using different RCMs and downscaling the same GCM (CAM), would possibly provide highly usefull information.

[30] see Section3.4

[31] Nesting is the implementation of additional grids with finer spatial and temporal resolutions into a parent grid with coarser resolution (Wang et al., 2007)

[32] Sylla et al.( 2011) is an initial study with the perpose of eventually downscaling CAM by RegCM3.

# Chapter 5

# Summary and conclusion remarks

This study investigates how WRF performs as a dynamical downscaler for CAM, by focusing on precipitation patterns over southern Africa. WRF has been initialised by CAM and land surface data from CLM, and every 6 hours forced by SSTs and at the lateral boundaries by CAM. The physical schemes were chosen from the range of alternatives that WRF provides: YSU (PBL), Kain-Fritsch (convective parametrization), CAM radiation (short and longwave), NOAH (LSM) and Lin. et al (microphysics). A historical run for 1990-2009 has been performed, analysed and discussed, with the aim of outlining WRF's capabilities of reproducing different precipitation patterns (seasonal, interannual, annual and extreme). In addition some preliminary results from a testrun for the future (2050-2069) have been shown, as well as shorter sensitivity runs using alternative physical scheme options.

Previous studies in southern Africa show that precipitation in RCMs share some of the same biases as the forcing data (GCMs or reanalysis)(Arnell et al., 2003; Engelbrecht et al., 2008; Hudson and Jones, 2002; Sylla et al., 2010), thus further development is needed. In Hudson and Jones (2002), the precipitation in the GCM simulation was generally closer to observed values than the downscaled precipitation from the RCM (both forced with GCM and reanalysis data), especially in the summer season. Although WRF has a larger bias than CAM in a few regions in summer, WRF (RCM) generally reproduces the seasonal rainfall patterns somewhat better than CAM (GCM), which implies that the results in this thesis are of relatively good or even better quality compared Hudson and Jones (2002). Note that different domain size, resolution etc. also influence the RCM results, thus any conclusions can not be drawn from comparing the results in this study to Hudson and Jones (2002).

Dynamical downscaling of precipitation over southern Africa are obviously complicated, but one have to keep in mind that this research is still

in its early phase, and that the possibilities of advancements are large. Obtaining higher resolution and better quality model data is necessary to produce regional climate projections, and an opportunity to achieve this lies within dynamical downscaling of GCMs by RCMs. Although the rainfall bias in WRF are not substantially less than in CAM, this study seems to make progress compared to previous work. Additionally, as the verification of the precipitation is in this study generally computed over large grid-averaged areas to compare with coarse resolution observational data, it captures mostly large scale precipitation. Therefor the additional information that WRF holds on a local scale, generally due to being more influenced by regional topography, is less evident in the presented results. As there are great potentials in dynamical downscaling of GCMs using RCMs, one should continue to strive for further improvements of the models, and regional climate modeling will possibly be taken to a next level with extended computational resources .

In this thesis, WRF reproduces the main features of seasonal and annual precipitation patterns satisfactorily. The distinct precipitation changes associated with the seasonal movement of ITCZ are well captured, and the different climatic zones are clearly visible. Nevertheless, WRF overestimates the precipitation intensity in the summer months, especially in the Mozambique Channel and on the southen African plateau. Many factors are probably contributing to the wet bias and it is difficult to account for them without targeted studies. Though a possible cause are a too strong low-level convergence over Angola (Angola high) in WRF, leading to a strengthend Walker circulation and a positive precipitation feedback mechanism, which also provides enhanced moisture for the rainbands stretching over the southern continent.

In the winter WRF successfully reproduces the low precipitation intensity over the continent, but fails to fully capture the precipitation rise associated with the winter rainfall season in southwestern Africa. The southward displacement of the Kalahari High, compared to observational data, possibly suppresses the westerlies and cut of lows which normally produce the winter precipitation here, and is suggested to result in the underestimations of precipitation on the southern tip in WRF.

WRF is generally slightly closer to observed mean precipitation compared to CAM from October to March, implying that dynamical downscaling by WRF slightly improves the CAM results on regional levels. Both models give a fairly good representation of the winter months (except southwestern Africa). WRF seems to reasonably capture the amplitude of the interannual rainfall variability, but the correlations between mean seasonal precipitation in observations and WRF are low, suggesting that SST anomalies are not the governing driving force behind interannual variability in most of southern Africa. However the correlations between CAM and GPCP for the summer season implies that over Namibia, Botswana and northern

South Africa, the interannual variability could to some degree be reproduced by models forced with observed SSTs. The extreme precipitation changes (R10, CDD, CWD and RR1_5) in WRF are reasonably simulated compared to observations, although some indices are displaced, and special regions deviates more than others ( western coast and Mozambique Channel).

Two additional shorter runs were performed and showed that varying physical scheme choices provided deviating results for the summer season. In each run, one scheme option was changed: substituting YSU by MYJ (PBL scheme) and Kain-Fritsch by Grell (cumulus parametrization scheme from Kain-Fritsch). Kain-Fritsch coupled with YSU (the historical run) induce wet bias over the southern African plateau and in the Mozambique Channel in summer. MYJ results in a dry bias in the Mozambique Channel and on the northeastern continent and slightly less wet bias over the southern African plateau compared to the control run. Grell simulates precipitation on the southern plateau quite well, but has a negative bias on the northeastern continent, as well as a positive bias in the Indian Ocean. The three shorter runs are all biased over different areas, suggesting that there might not exist a "right" configuration representing the physical processes of every region of southern Africa. This assumption is supported by recent studies (Cretat et al., 2011).

Crètat et al (2011) performed 27 runs with WRF over a similar domain for different schemes during the summer season of 1993/1994 , forcing with reanalysis data(ERA40)[1]. The results presented in their study are analogue to this study concerning the conclusions drawn above, although the YSU scheme seems to produce the least precipitation of the two PBL schemes. It should be noted that this recent published article also contains valuable information for other choices of scheme options, which should be taken into consideration before future work suggested in section 4.6 are performed.

Simulations with RCMs will differ for various physical parametrization, size, location, seasons or forcing model, and one should have this in mind when comparing with results from former work. Nevertheless, this study seems to be in good agreement with previous studies, all generally successfully reproducing seasonal and annual variations, and overestimating precipitation in the summer season (Cretat et al., 2011; Sylla et al., 2011, 2010; Tadross et al., 2005; Engelbrecht et al., 2008; Giorgi et al., 2011; Hudson and Jones, 2002; Arnell et al., 2003). Overall, as RCMs will resolve more of the physical processes in large-scale precipitation and enhance the topographical forcing, it seems to produce a possibly too active hydrological cycle (Hudson and Jones, 2002). Sylla et al. (2011) forced RegCM3 over a similar domain with two different sets of global reanalysis data (NCEP and ERA-Interim), and obtained the same strong low-level convergence, neg-

[1]Crètat ran with a lower resolution (35 km x 35m) and different microphysical schemes

ative temperature bias, and wet bias over the Indian Ocean and the south-eastern plateau in both runs.

Overall, WRF is able to capture the observed seasonal and annual variability well. With further research and development, dynamical downscaling by the use of WRF can become a very important tool for providing climate change projections for the future. This thesis is unique in the way of exploring precipitation patterns over southern Africa, by forcing WRF with CAM, a leading model in the IPCC studies. Thus high quality downscaling of CAM can be of huge importance for future climate projections, as WRF can supply valuable high resolution quality data for instance for hydrological and agricultural applications.

# Appendix A

# Input of greenhousgasses to WRF

The Representative Concentration Pathway (RCP) are new greenhouse-scenarios from the IPCC. RCP4.5 is given as input for WRF and CAM in this study, which is a low-medium scenario of greenhouse gas emissions(Moss et al., 2010). Listed beneath are the concentrations for 1990-2009 and 2050-2069.

| Year | co2 (ppmv) | n2o (ppbv) | ch4 (ppbv) | cfc11 (ppbv) | cfc12 (pppbv) |
|---|---|---|---|---|---|
| 1990 | 353.855 | 309.485 | 1693.63 | 527.539 | 466.150 |
| 1991 | 355.018 | 310.113 | 1703.818 | 596.488 | 481.300 |
| 1992 | 355.885 | 310.602 | 1711.800 | 617.293 | 494.400 |
| 1993 | 356.778 | 311.078 | 1716.290 | 632.492 | 504.800 |
| 1994 | 358.128 | 311.603 | 1721.012 | 642.864 | 513.100 |
| 1995 | 359.838 | 312.295 | 1726.350 | 649.147 | 519.550 |
| 1996 | 361.463 | 313.048 | 1730.010 | 655.469 | 525.050 |
| 1997 | 363.155 | 313.760 | 1734.818 | 661.665 | 529.150 |
| 1998 | 365.323 | 314.533 | 1742.710 | 665.738 | 532.400 |
| 1999 | 367.348 | 315.258 | 1749.243 | 670.447 | 534.950 |
| 2000 | 368.865 | 315.850 | 1751.022 | 676.053 | 537.050 |
| 2001 | 370.468 | 316.488 | 1750.708 | 681.751 | 538.850 |
| 2002 | 372.523 | 317.245 | 1752.188 | 688.791 | 539.950 |
| 2003 | 374.760 | 318.018 | 1754.760 | 695.628 | 540.050 |
| 2004 | 376.813 | 318.710 | 1755.065 | 702.000 | 539.900 |
| 2005 | 378.813 | 319.440 | 1753.735 | 708.715 | 539.400 |
| 2006 | 380.900 | 320.400 | 1753.735 | 706.615 | 538.700 |
| 2007 | 382.700 | 321.100 | 1764.000 | 704.315 | 537.100 |
| 2008 | 384.800 | 322.100 | 1774.000 | 702.315 | 534.600 |
| 2009 | 386.270 | 322.900 | 1784.000 | 700.115 | 532.200 |
| 2050 | 486.535 | 350.608 | 1833.094 | 724.225 | 347.834 |
| 2051 | 489.060 | 351.211 | 1831.276 | 712.606 | 343.695 |
| 2052 | 491.536 | 351.807 | 1829.210 | 701.319 | 339.592 |
| 2053 | 493.932 | 352.396 | 1826.776 | 690.331 | 335.526 |
| 2054 | 498.474 | 353.553 | 1820.661 | 669.283 | 327.481 |
| 2055 | 498.474 | 353.553 | 1820.661 | 669.283 | 327.481 |
| 2056 | 500.645 | 354.120 | 1817.052 | 659.255 | 323.502 |
| 2057 | 502.768 | 354.681 | 1813.175 | 649.582 | 319.558 |
| 2058 | 504.847 | 355.235 | 1809.091 | 640.275 | 315.653 |
| 2059 | 506.884 | 355.782 | 1804.863 | 631.341 | 311.789 |
| 2060 | 508.871 | 356.322 | 1800.511 | 622.776 | 307.968 |
| 2061 | 510.799 | 356.856 | 1796.029 | 614.567 | 304.187 |
| 2062 | 512.647 | 357.382 | 1791.340 | 606.763 | 300.446 |
| 2063 | 514.402 | 357.901 | 1786.382 | 599.409 | 296.743 |
| 2064 | 516.065 | 358.412 | 1781.178 | 592.484 | 293.080 |
| 2065 | 519.096 | 359.409 | 1769.852 | 579.790 | 285.848 |
| 2066 | 519.096 | 359.409 | 1769.852 | 579.790 | 285.848 |
| 2067 | 520.488 | 359.897 | 1763.787 | 573.984 | 282.279 |
| 2068 | 521.818 | 360.377 | 1757.545 | 568.527 | 278.746 |
| 2069 | 523.089 | 360.849 | 1751.177 | 563.407 | 275.252 |

# Appendix B

# Interannual variability of seasonal precipitation

Presented here are area-averaged mean seasonal (DJF and JJA) interannual variability precipitation over each region of the southern African contintent.

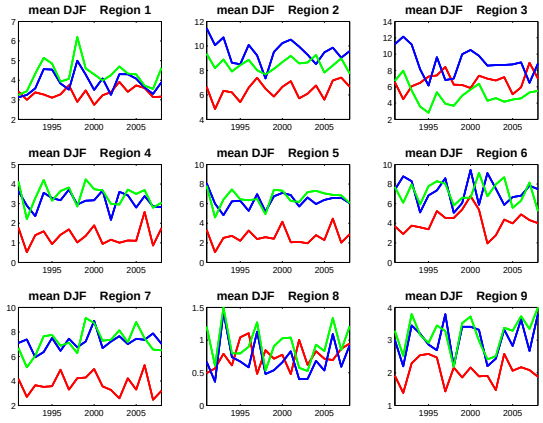


**Figure B.1:** *Area-averaged interannual variability of summer (DJF) precipitation (mm/day) for each region. Blue =WRF, green =CAM, red = GPCP.*

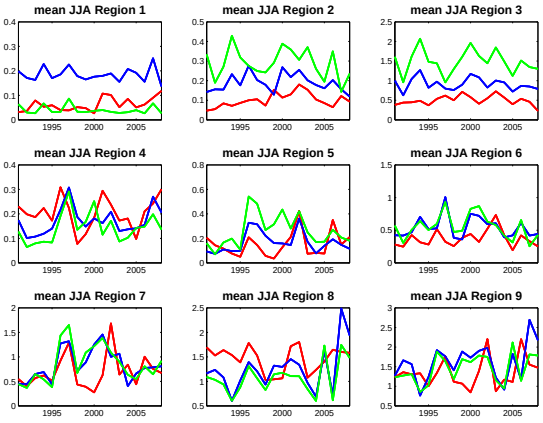


**Figure B.2:** *Area-averaged interannual variability of winter (JJA) precipitation (mm/day) for each region. Blue =WRF, green =CAM, red = GPCP.*

# Appendix C

# Trends for 1998-2009 in TRMM

Trends calculated from TRMM data using the same method as described in Section 4.4. Provided by Sandeep Sukumaran (Sukumaran, 2011).

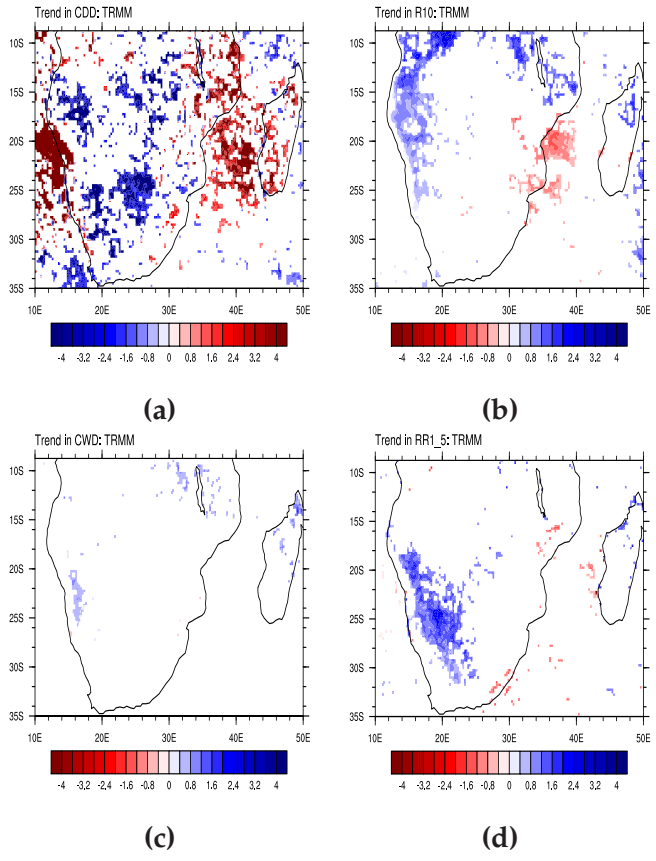


**Figure C.1:** *Trends (number of days/year) in TRMM for 1998-2009, calculated on a 90% significants level for a) CDD, b) R10, c)CWD and d)RR1_5.*

# Bibliography


Adler, RF; Huffman, GJ; Chang, A; Ferraro, R; Xie, PP; Janowiak, J; Rudolf, B; Schneider, U; Curtis, S; Bolvin, D; Gruber, A; Susskind, J; Arkin, P and Nelkin, E (2003) *T*he version-2 global precipitation climatology project (GPCP) monthly precipitation analysis (1979-present). American Meteorogical Society.

Arnell, N. W.; Hudson, D. A. and Jones, R.G. (2003) *C*limate change scenarios from a regional climate model: Estimating change in runoff in southern Africa. Vol. 108.

Bell, Jason L.; Sloan, Lisa C. and Snyder, Mark A. (2003) *R*egional Changes in Extreme Climatic Events. American Meteorological Society.

Boko, M.; Niang, I.; Nyong, A.; Vogel, C.; Githeko, A.; Medany, M.; Osman-Elasha, B.; Tabo, R. and Yanda, P. (2007) *A*frica- Climate Change. In *I*mpacts, Adaptation and Vulnerability. Contribution of Working Group II to the Fourth Assessment Report of the Intergovernmental Panel on Climate Change, M.L. Parry, O.F. Canziani, J.P. Palutikof, P.J. van der Linden and C.E. Hanson, Eds. (Cambridge University Press, Cambridge, United Kingdom).

Bukovsky, Melissa S. and Karoly, David J. (2009) *P*recipitation Simulations Using WRF as a Nested Regional Climate Model. Journal of applied meteorology and climatology.

Caldwell, Peter; S., Hung-Neng Chin and C.Bader, David (2009) *E*valuation of a WRF dynamical simulation over California. Climatic Change, p. 499–521.

Christensen, J.H; Hewitson, B.; A. Busuioca ndA. Chen, X. Gao; Held, I.; Jones, R.; Kolli, R.K.; Kwon, W.-T.; Laprise, R.; Rueda, V. Magaña; Mearns, L.; Menéndez, C.G.; Räisänen, J.; Rinke, A.; Sarr, A. and Whetton, P. (2007) *U*nderstanding and Attributing Climate Change.. In *C*limate Change 2007: The Physical Science Basis. Contribution of Working Group I to the Fourth Assessment Report of the Intergovernmental Panel on Climate Change [Solomon, S., D. Qin, M. Manning, Z. Chen, M. Marquis, K.B. Averyt, M. Tignor and H.L. Miller (eds.)] (Cambridge University Press, Cambridge, United Kingdom and New York, NY, USA).

Compo, GP; Whitaker, JS and Sardeshmukh, PD (2006) *F*easibility of a 100-year reanalysis using only surface pressure data. Bulletin of the american meteorological society, Vol. 87(2).

Cretat, Julien; pohl, Benjamin; Richars, Yves and Drobenski, Philippe

(2011) *U*ncertanties in simulationg regional climate of Souhtern Africa: sensitiviy to phsyical paramtersizations using WRF. Climate Dynamics.

Davies, E.G.R. and Simonovic, S.P. (2005) *C*limate change and the hydrological cycles.

Engelbrecht, F. A.; McGregor, J. L. and Engelbrecht, C. J. (2008) *D*ynamics of the Conformal-Cubic Atmospheric Model projected climate-change signal over southern Africa. International journal of climatology, p. 1013–1033.

Fernandez, Jesús (2010) *C*ORDEXrelated activitities at the Santander Meteorology Group (Universidad de Cantabria). [online] `http://www.meteo.unican.es`.

Fita, L.; Fernàndez, J. and Garcìa-Dìez, M. (2010) *C*LWRF: WRF modifications for regional climate simulation under future scenarios. Grupo de Meteorologia, Dpt. Appl. Math. and Comp. Scie., Universidad de Cantabria.

Flaounas, Emmanouil; Bastin, Sophie and Janicot, Serge (2010) *R*egional climate modelling of the 2006 West African monsoon: sensitivity to convection and planetary boundary layer parameterisation using WRF. Springer Verlag.

Frich, P.; Alexande, L.V.; Della-Martha, P.; Gleason, B. and Haylock, M. (2002) *O*bserved coherent changes in climatic extremes during second half of the twentieth century. Climate research, p. 193–212.

Giorgi, F; Coppola, E.; Solomon, F.; Mariotti, L. and Sylla, M. (2011) *R*egCM4: Model descprition and prelimiary tests over multiple CORDEX domains.

Giorgi, Filippo; Brouder, Christine Shields and Bastes, Gary T. (1994) *R*egional Climate Change Scenarios over the United States Produced with a Nested Regional Climate Model. American Geophysical Union, p. 375–399.

Giorgi, Filippo and Mearns, Linda O. (1991) *A*pproaches to the simulation of regional climate change: a review. American Geophysical Union, p. 191–216.

Gochis, David J.; Shuttleworth, James and Yang, Zong-Liang (2002) *S*ensitivity of the modeled North American monsoon regional climate to convective parameterization. Monthly weather review, Vol. 130.

Gunwald, G.K and Jones, R.H (2000) *M*arkov models for time series with mixed distribution. Environmetrics, Vol. 11.

Hart, N. C. G.; Reason, C. J. C. and Faufhereau, N. (2010) *T*ropical-Extratropical interactions over Southern Africa: Three cases of heavy summer season rainfall. Americal Meterological Sosciety.

Hartmann (1994) *G*lobal Physical Climatology.

Holland, Greg J.; Done, James and Bruyere, Cindy (2011) *M*odel Investigations of the Effects of Climate Variability and Change on Future Gulf of Mexico Tropical Cyclone Activity. Copyright 2010, Offshore Technology Conference.

Hudson, D. A. and Jones, R.G. (2002) *R*egional climate model simulations of present-day and future climates of southern Africa. Met Office, Hadley Center for Cliamte Prediction and Research, London Road.

Huffmana, George J and Bolvin, David T. (2009) *G*PCP Versjion 2.1 Combined Precipiation Data Set Documentation. Laboarory for Atmoshere.

IPCC (2007) *R*egional Climate Projections. In *C*limate Change 2007: The Physical Science Basis. Contribution of Working Group I to the Fourth Assessment Report of the Intergovernmental Panel on Climate Change. [Solomon, S., D. Qin, M. Manning, Z. Chen, M. Marquis, K.B. Averyt, M. Tignor and H.L. Miller (eds.)] (Cambridge University Press, Cambridge, United Kingdom and New York, NY, USA).

J. L Privette, G. Robert S R. J Scholes Y. Wang K.K Caylor P.F Ros M Mukelabai, Y. Titan (2004) *V*egetation structure characteristics and relationships of Kalahari woodlands and savannas. American Meteorlogical Society, Vol. 10: p. 281–291.

Jones, Peter G. and Thornton, Philip K. (2003) *T*he potential impacts of climate change on maize production in Africa and Latin America in 2055.. Elsevier Science.

Jury, MR (2002) *E*conomic impacts of climate variability in South Africa and development of resource prediction models. Journal of applied meteorology, Vol. 41(1): p. 46–55.

Landman, Wilhelm A.; Seth, Anji and Camargo, Suzana J. (2005) *T*he effect of regional climate model domain choice on the simulation of tropical cyclone-like vortices in the Southwestern Indian oceanS.

Layberry, R. and Kniveton, D.R (2000) *P*recipitation over Southern Africa: A New Resource for Climate Studie. Journal of hydrometeorology.

Little, M. A.; McSharry, P. E. and Taylor, J. W. (2009) *G*eneralized Linear Models for Site-Specific Density Forecasting of UK Daily Rainfall. Monthly weather review, Vol. 137.

Lo, Jeff Chun-Fung; Yang, Zong-Liang and Sr., Roger A. Pielke (2008) *A*ssessment of three dynamical climate downscaling methods using the Weather Research and Forecasting (WRF) model. Journal of Geophysical Research, Vol. 113.

Mason, S. J. and Jury, M.R. (1997) *C*limatic variability and change over southern Africa: a reflection of underlying processes. Progress in physical geography, Vol. 21: p. 23–50.

McHugh, Maurice J. and Rogers, Jefrey C. (2001) *N*orth Atlantic oscillation influence on precipitation variability around the Southeast African Convergence Zone. Journal of Climate, Vol. 14: p. 3631–3642.

Mesquita, Michel; Lunde, Torleif and Bader, Jürgen (2010) *E*asterly Waves in Tropical Channel Simulations. Lecture notes from WRF lecture series at Bjerknes Center in Bergen.

Moss, Richard H.; Edmonds, Jae A.; Hibbard, Kathy A.; Manning, Martin R.; Rose, Steven K.; van Vuuren, Detlef P.; Carter, Timothy R.; Emori, Seita; Kainuma, Mikiko; Kram, Tom; Meehl, Gerald A.; Mitchell,

John F. B.; Nakicenovic, Nebojsa; Riahi, Keywan; Smith, Steven J.; Stouffer, Ronald J.; Thomson, Allison M.; Weyant, John P. and Wilbanks, Thomas J. (2010) *T*he next generation of scenarios for climate change research and assessment. Nature, Vol. 463: p. 747–756.

Murthi, Aditya; Bowman, Kenneth P. and Leung, L. Ruby (2010) *S*imulations of precipitation using NRCM and comparisons with satellite observations and CAM: annual cycle. Climate dynamics.

Qian, Yun; Ghan, Steven J. and Leung, L. Ruby (2010) *D*ownscaling hydroclimatic changes over the Western US based on CAM subgrid scheme and WRF regional climate simulations. International journal of climatology, Vol. 30: p. 675–693.

Reason, C. J. C.; Landman, W. and Tennant, W. (2006) *S*easonal to Decadal Prediction of Southern African Climate and Its Links with Variability of the Atlantic Ocean.

Reason, C. J. C. and M.Rouault (2005) *L*inks between the Antarctic Oscillation and winter rainfall over western South Africa. Geophysical Research letters, Vol. 32.

Rogers, R. R and Yau, M. K. (1989) *A* short course in cloud physics (Butterworth Heinemann, Elsvier).

Seth, Angi and Giorgi, Filippo (1998) *T*he Effects of Domain Choice on Summer Precipitation Simulation and Sensitivity in a Regional Climate Model. Journal of climatology, Vol. 11: p. 2698–2712.

Shugart, H. H.; Macko, S. A.; Lesolle, P.; Szuba, T. A.; Mukelabai, M. M.; Dowty, P. and Swap, R. J. (2004) *T*he SAFARI 2000 - Kalahari Transect Wet Season Campaign of year 2000. Global change biology, Vol. 10.

Skamarock, William C. and Klemp, Joseph B. (2008) *A* time-split nonhydrostatic atmospheric model for weather research and forecasting applications. Journal of computational physics.

Skamarock, William C.; Klemp, Joseph B.; Dudhia, Jimy; Gill, David O.; Barker, Dale M.; Wang, Wei and Powers, Jordan G. (2007) *A* Description of the Advanced Research WRF Version 2. Technical report.

Stringer, Lindsay C.; Dyer, Jen C.; Reed, Mark S.; Dougill, Andrew J.; Twyman, Chasca and Mkwambisi, David (2009) *A*daptations to climate change, drought and desertification: local insights to enhance policy in southern Africa. Enviornmental Science and Policy, Vol. 12: p. 748–765.

Sukumaran, Sandeep (2011) *R*ecent Changes in the Wet and Dry Patterns Detected in TRMM Precipitation Data. sumbitted to Journal of Applied Meteorology and Climatology.

Svendsen, Mark; Exing, Mandy and Msangi, Siwa (2008) *A*frica infrastructure country diagnostic. International Food Policy Research Institute for the World Bank.

Sylla, Mouhamadou Bamba; Coppola, E.; Mariotti, L.; Giorgi, F.; Ruti, P. M.; Dell'Aquila, A. and Bi, X. (2010) *M*ultiyear simulation of the African climate using a regional climate model (RegCM3) with the high resolution ERA-interim reanalysis. Climate dynamics, Vol. 35: p. 231–247.

Sylla, Mouhamadou Bamba; Giorgi, F. and Stordal, F. (2011) *T*he large-scale origins of rainfall bias and their link to surface radtaion in high resoulation simulations over Southern Africa. submitted.

Tadross, Mark; Jack, Chris and Hewitson, Bruce (2005) *S*ON RCM-based projections of change in southern African summer climate. Geophysical Research Letters, Vol. 32.

Taljaard, J. T. (1998) *C*hange of rainfall distribution and circulation patterns over southern Africa in summer. International journal of climatology.

Todd, M. and Washington, R. (1999) *C*irculation anomalies associated with tropical-temperate troughs in southern Africa and the south west Indian Ocean. Climate Dynamics, Vol. 15: p. 937–951.

Tummon, Fiona (2011) *D*irect and semi-direct aerosol effects on the southern African regional cliamte during the asutral winter season. Sumbittet PhD.

Tyson, PD and Preston-Whyte, RA (2000) *T*he Weather and Climate of Southern Africa (Oxford University Press).

UCAR-edu () *E*SSL LAR 2008: Strategic Goal. [online] `http://www.nar.ucar.edu/2008/ESSL/sp3/images/sp3_07_mm_1.jpg`, month = , year = 2008,.

UCAR-edu (2010) *H*ow Models Produce Precipiation and Clouds. [online] `http://www.meted.ucar.edu/nwp/model_precipandclouds/print.htm`.

UNEP (2006) *C*limate variability and cliamte change in southern Africa.

Venkata, Srinivas Challa; Jayakumar, Indracanti; Rabarison, Monika; Patrick, Chuck; Baham, Julius; Young, John; Hughes, Robert; Hardy, Mark; Swanier, Shelton; Yerramilli, Anjaneyulu; Aditya, Murthi; Bowman, Kenneth P. and Ruby, Leung L. () .

Wallace, John .M and Hobbs, Peter V. (2006) *A*tmospheric science -an introductory survey.

Wang, Wei; Bruyère, Cindy; Duda, Michael; Dudhia, Jimy; Gill, Dave; Michalakes, John and Zhang, Syed Rizviand Xin (2007) *A*RW Version 3 Modeling System User's Guide. Mesoscale and Microscale Meteorology Division, National Center for Atmospheric Research, Boulder, Colorado, USA.